Stem Cell Reports
Article

OPEN ACCESS

HOXB4 Promotes Hemogenic Endothelium Formation without Perturbing Endothelial Cell Development

Nadine Teichweyde,[1] Lara Kasperidus,[1,2] Sebastian Carotta,[3] Valerie Kouskoff,[4] Georges Lacaud,[5] Peter A. Horn,[1] Stefan Heinrichs,[1] and Hannes Klump[1,*]

[1]Institute for Transfusion Medicine, University Hospital Essen, Virchowstraße 179, 45147 Essen, Germany
[2]Department of Bone Marrow Transplantation, University Hospital Essen, Hufelandstraße 55, 45147 Essen, Germany
[3]Cancer Cell Signaling, Boehringer Ingelheim RCV, Dr Boehringer-Gasse, 1120 Vienna, Austria
[4]Cancer Research UK Stem Cell Haematopoiesis Group
[5]Cancer Research UK Stem Cell Biology Group
Cancer Research UK Manchester Institute, The University of Manchester, Wilmslow Road, Manchester M20 4BX, UK
*Correspondence: hannes.klump@uk-essen.de
https://doi.org/10.1016/j.stemcr.2018.01.009

SUMMARY

Generation of hematopoietic stem cells (HSCs) from pluripotent stem cells, *in vitro*, holds great promise for regenerative therapies. Primarily, this has been achieved in mouse cells by overexpression of the homeotic selector protein HOXB4. The exact cellular stage at which HOXB4 promotes hematopoietic development, *in vitro*, is not yet known. However, its identification is a prerequisite to unambiguously identify the molecular circuits controlling hematopoiesis, since the activity of HOX proteins is highly cell and context dependent. To identify that stage, we retrovirally expressed HOXB4 in differentiating mouse embryonic stem cells (ESCs). Through the use of *Runx1*$^{(-/-)}$ ESCs containing a doxycycline-inducible *Runx1* coding sequence, we uncovered that HOXB4 promoted the formation of hemogenic endothelium cells without altering endothelial cell development. Whole-transcriptome analysis revealed that its expression mediated the upregulation of transcription of core transcription factors necessary for hematopoiesis, culminating in the formation of blood progenitors upon initiation of *Runx1* expression.

INTRODUCTION

Patient-specific, induced pluripotent stem cells (iPSCs) present an attractive starting point for generation of autologous hematopoietic stem cells (HSCs) for treating certain hematologic diseases in the future (Klump et al., 2013; Wahlster and Daley, 2016). However, directed differentiation toward HSCs has remained inefficient, indicating that some key requirements necessary for full hematopoietic specification, *in vitro*, are still ill-defined, likely owing to our incomplete knowledge of HSC development, *in vivo*.

During embryonic development, definitive, multipotent HSCs are formed by a subset of cells lining the ventral floor of the dorsal aorta termed hemogenic endothelial (HE) cells (Bertrand et al., 2010; Jaffredo et al., 1998; Tavian et al., 2001; Zovein et al., 2010). Endothelial and blood cells share a similar gene expression pattern and emanate from common mesodermal progenitors (Kataoka et al., 2011; Liu et al., 2013; Wareing et al., 2012). When isolated from embryos or differentiating embryonic stem cell (ESC) cultures, these progenitors, so-called hemangioblasts, form blast colonies, *in vitro*, containing both endothelial and hematopoietic progenitors (Choi et al., 1998; Kennedy et al., 1997), and, in some reports, even smooth muscle cells (Ema et al., 2003). During blast colony formation, HE cells are generated as intermediate cells, which subsequently undergo endothelial-to-hematopoietic transition (EHT) (Lancrin et al., 2009).

Several transcription factors (TFs) are known to be important intrinsic regulators of endothelial as well as HSC development, such as SCL/TAL1, ETV2, GATA2, or MEIS1 (Azcoitia et al., 2005; Bloor et al., 2002; Liu et al., 2012, 2015). However, for the enforced generation of sufficient numbers of HSCs from differentiating pluripotent stem cells, *in vitro*, the instructive regulatory networks controlling separation of the endothelial and hematopoietic lineages and the critical time points of their action need to be identified. Single-cell transcriptional profiling during early mesoderm development has turned out to be a key approach for this purpose, allowing for an improved distinction of endothelial cells and hematopoietic progenitors during early mesodermal differentiation (Moignard et al., 2015; Scialdone et al., 2016; Swiers et al., 2013). Some of the identified hematopoiesis-associated genes are involved in a regulatory network controlling *Runx1* transcription, which is essential for the formation of adult definitive HSCs by directly controlling EHT (Lacaud et al., 2002; Lancrin et al., 2009; North et al., 1999). Because only limited numbers of HSCs are present in embryos (Taoudi et al., 2008), the availability of HE cells may be a crucial bottleneck for the *de novo* generation of HSCs. Therefore, adequate numbers of HE cells likely need to be generated for the formation of sufficient numbers of HSCs, *in vitro*.

Except one report describing the development of hematopoietic stem and progenitor cells (HSPCs) from genetically unmanipulated ESCs (Pearson et al., 2015), significant and

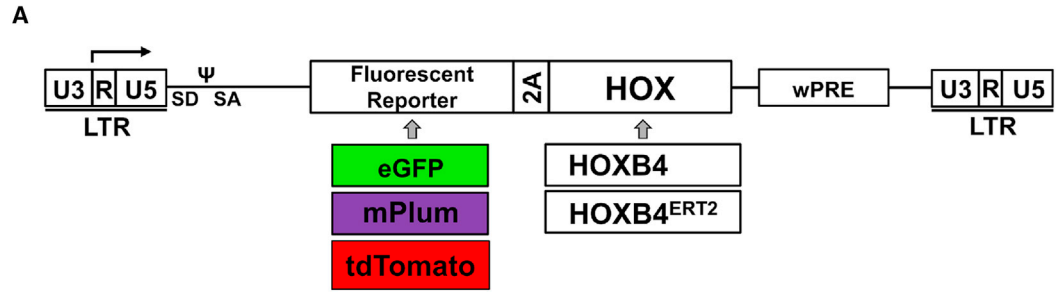

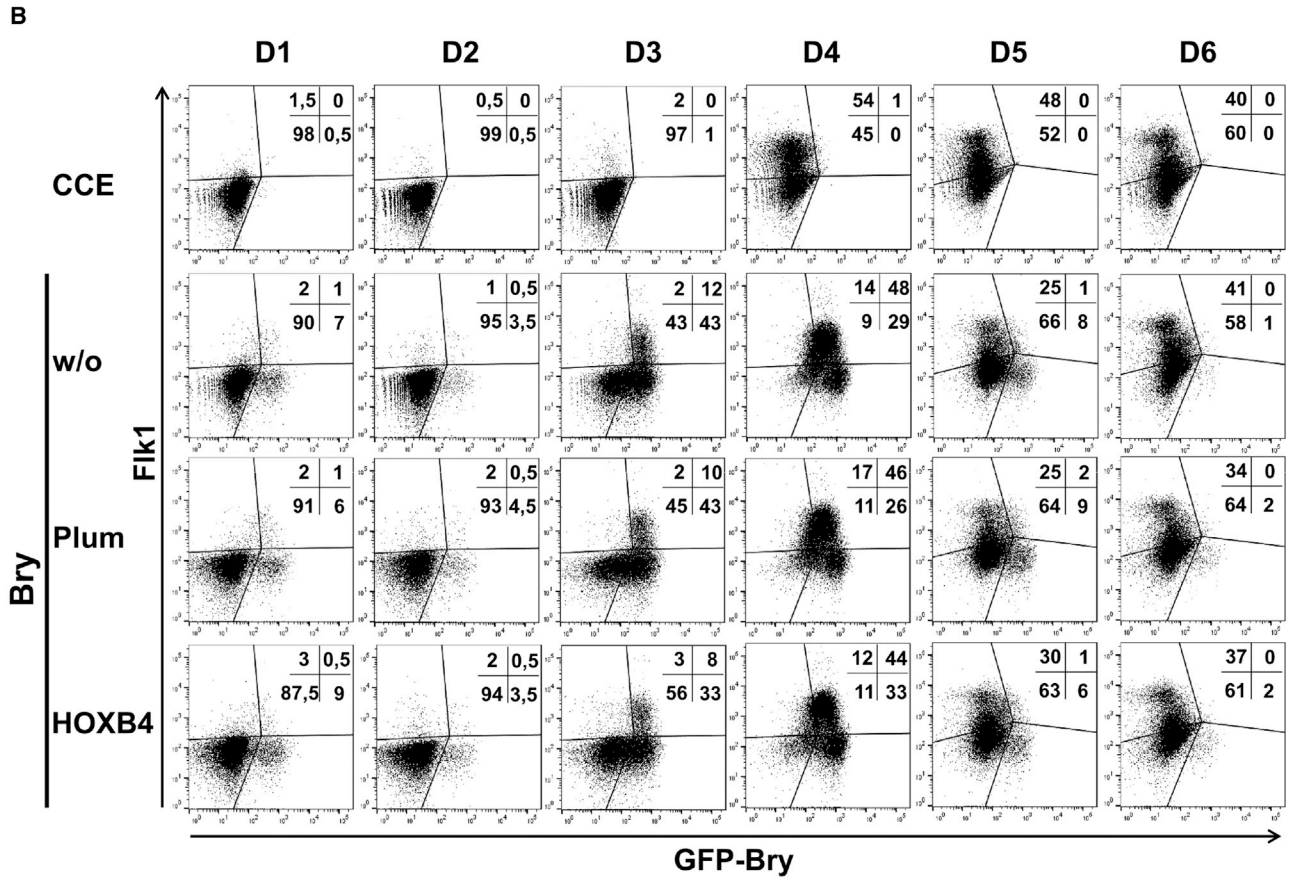

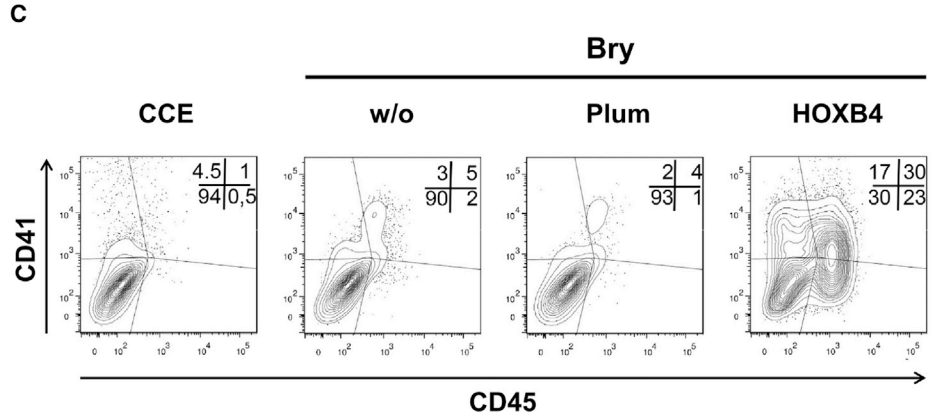

(legend on next page)

stable long-term repopulation of pluripotent stem cell-derived HSPCs has only been achieved using mouse cells, and only when the homeotic selector protein HOXB4 was ectopically expressed (Chan et al., 2008; Kyba et al., 2002; Lesinski et al., 2012; Lu et al., 2016; Pilat et al., 2005). However, differentiation of transplanted HSPCs was skewed toward myelopoiesis with a concomitant inhibition of lymphopoiesis and erythropoiesis in a dose-dependent manner, suggesting either an incomplete maturation of ESC-derived HSPCs and/or active interference with transcriptional circuitries controlling differentiation (Kyba et al., 2002; Pilat et al., 2005; Schiedlmeier et al., 2003). Although we, and others, have identified target genes of HOXB4 in differentiating mouse ESCs (Fan et al., 2012; Jackson et al., 2012; Oshima et al., 2011; Schiedlmeier et al., 2007), these findings have not yet led to a satisfying explanation on how HOXB4 promotes HSPC development, *in vitro*. The most likely reason is that the activities of HOX proteins, as modulators of transcription, are highly context dependent and influenced by the microenvironment of a given cell (Abate-Shen, 2002; Schiedlmeier et al., 2007; Will et al., 2006). So far, the cellular stage at which HOXB4 unfolds its activities during hematopoiesis, *in vitro*, is not yet known. Thus, its identification would be a prerequisite for unambiguously identifying the key molecular circuitries driving hematopoietic development and for the *in vitro* generation of HSPCs from pluripotent stem cells.

In this work, we demonstrate that HOXB4 promotes the generation of early hematopoietic progenitors from differentiating mouse ESCs, *in vitro*, by enforcing the development of HE cells poised for the induction of EHT by RUNX1. Molecularly, it does so, at least in part, by upregulating the expression of key TFs involved in hematopoietic development.

RESULTS

Ectopic HOXB4 Expression Does Not Promote Mesoderm Specification

As hematopoietic cells originate from the mesoderm, we transduced *Brachyury* (Bry) reporter ESCs (GFP-Bry, kindly provided by J. Fehling, Ulm) (Fehling et al., 2003) with retroviral vectors co-expressing HOXB4 and the fluorescent protein mPlum (Figure 1A), and determined GFP as well as vascular endothelial growth factor receptor 2 (FLK-1) expression during differentiation (Nishikawa et al., 1998). The peak of $Bry^{GFP+}FLK\text{-}1^{+}$ cells was detected between days 3 and 4 of embryoid body (EB) development, *in vitro*. At this stage of development, ectopic expression of HOXB4 did not promote specification of $Bry^{GFP+}FLK\text{-}1^{+}$ mesodermal cells (Figure 1B). Later, however, HOXB4 strongly enhanced the formation of $CD41^{+}$ and $CD45^{+}$ hematopoietic progenitors after dissociation of EB day 6 GFP-Bry (EBd6) cells and subsequent co-culture on OP9 stromal cells, confirming our previous results with CCE ESCs (Figures 1C and S1; Movie S1) (Chan et al., 2008; Lesinski et al., 2012). These results indicate that HOXB4 first acts downstream of early mesoderm specification and upstream of hematopoietic progenitor formation during differentiation of pluripotent stem cells.

HOXB4 Promotes Formation of a Hemogenic Endothelium

Concomitant to the marked formation of ESC-derived $CD41^{+}$ and $CD45^{+}$ progenitors in OP9 co-cultures, ectopic HOXB4 led to an increased number of adherent circular structures, which were associated with suspension cell clusters (Figure 2A), expressed VE-cadherin, CD31, and were capable of acetylated low-density lipoprotein uptake (Figures 2B and 2C). The suspension cells continued to proliferate only when HOXB4 was ectopically expressed and, after transplantation into immunodeficient NSG mice, mediated the typical pattern of myeloid-biased repopulation, as repeatedly reported by us and others (Figures S2A–S2D) (Kyba et al., 2002; Lesinski et al., 2012; Lu et al., 2016; McKinney-Freeman et al., 2009; Pilat et al., 2005; Wang et al., 2005). The adherent circular, cobblestone-like structures were reminiscent of previously described HE colonies (Eilken et al., 2009; Lancrin et al., 2009). To test this notion, we used a *Runx1* knockout ESC line carrying a doxycycline-inducible *Runx1* coding sequence stably integrated into the genome (iRunx cells)

Figure 1. HOXB4 Does Not Promote Early Mesoderm Specification, *In Vitro*

(A) Scheme depicting the gammaretroviral, FMEV-based expression vectors (Lesinski et al., 2012; Schiedlmeier et al., 2007). The vectors co-express a fluorescent protein (eGFP, mPlum, or tdTomato) together with HOXB4 or a 4-hydroxytamoxifen (Tam) inducible form, $HOXB4^{ERT2}$. Co-translational separation of the proteins is mediated by the TAV-2A esterase. LTR, long terminal repeat; wPRE, woodchuck hepatitis virus posttranscriptional regulatory element.

(B) Vector-transduced GFP-Bry ESCs (mPlum +/− HOXB4) were differentiated as embryoid bodies (EBs). At the indicated days, eGFP fluorescence as well as FLK-1 expression were determined by flow cytometry. The percentages of $eGFP^{+}FLK\text{-}1^{+}$ cells are shown. CCE ESCs were used as eGFP-negative controls (top row).

(C) After 6 days of differentiation, GFP-Bry EBs were dissociated and 10^{5} cells each co-cultured on OP9 stoma cells for further 8 days. Contour plots of flow cytometry analysis are shown, the percentages of $CD41^{+}$ and $CD45^{+}$ cells are indicated. For (B) and (C), representative results of n = 3 independent experiments are shown.

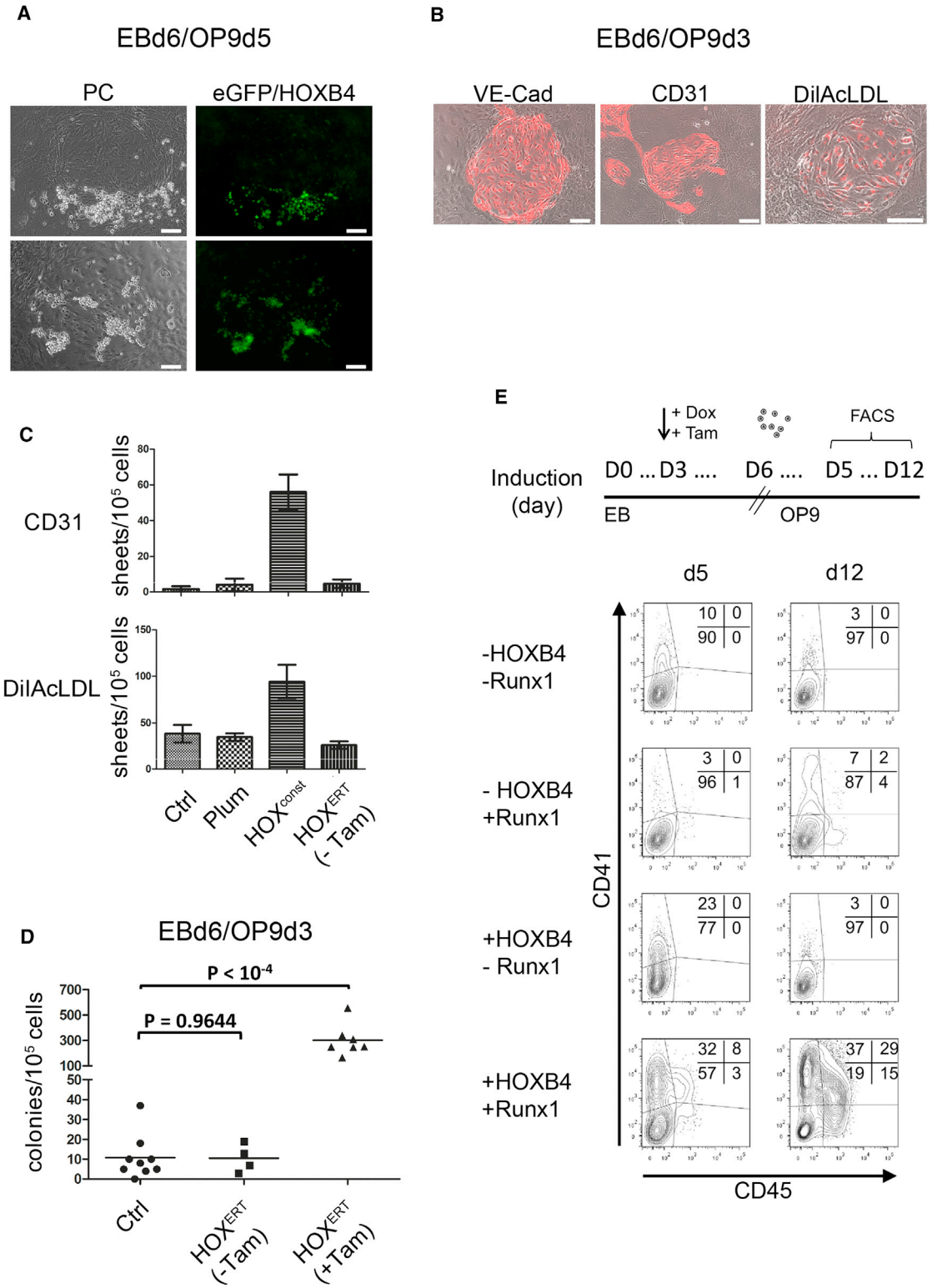

Figure 2. Formation of HE Colonies Is Promoted by HOXB4

(A) During co-culture on OP9 cells, circular sheet colonies were formed by the dissociated CCE-ESC-derived EBs (eGFP-HOXB4 transduced), which were commonly associated with hematopoietic suspension cell clusters. Left panel: phase contrast; right panel: eGFP-fluorescence. Scale bars, 100 μm.

(legend continued on next page)

(Lancrin et al., 2009). These cells are blocked immediately prior to EHT due to the absence of *Runx1* expression, which is essential for transition of the HE to hematopoietic cells. Importantly, the induction of its expression rescues the generation of blood cells (Lancrin et al., 2009). This system allowed us to answer the question of whether HOXB4 acts upstream of *Runx1* in promoting the hematopoietic fate and to separate RUNX1-dependent from RUNX1-independent effects of HOXB4, as well. HOXB4 overexpression in the absence of RUNX1 led to a significant accumulation of endothelial colonies (Figure 2D). To test if these cells are truly hemogenic, we induced *Runx1* expression by addition of doxycycline to the cultures (Movie S2). After *Runx1* induction, EHT of the endothelium cells initiated with a concomitant strong upregulation of CD41 expression, particularly when HOXB4 was activated (Figure 2E). Between day 5 and 12, a subpopulation of $CD41^+$ cells also initiated $CD45^+$ expression and continued to mature toward $CD41^-CD45^+$ cells. Without *Runx1* induction, the proportion of cells expressing low levels of CD41 was also strongly increased by HOXB4. However, these cells did not undergo EHT, further upregulate CD41 expression, or even generate $CD45^+$ cells. Instead, the proportion of $CD41^+$ cells strongly diminished over time. Without ectopic human HOXB4, a much smaller proportion of cells became $CD41^+$ or $CD45^+$ after induction of *Runx1*, which was in line with the significantly reduced number of HE colonies present in the cultures. Moreover, transcription of the hemato-endothelial genes *Scl/Tal1*, *Gata2*, *Lmo2*, and *Cdh5* (encoding VE-cadherin) and *Pecam1* (Gritz and Hirschi, 2016) was upregulated by HOXB4 in the absence of *Runx1* (Figure S3B). After induction of *Runx1*, expression of the key hematopoietic TF *Pu.1* (Iwasaki et al., 2005) was induced, as well as *Gfi1* and *Gfi1b*, two direct downstream effectors of RUNX1, which are necessary for the early and late phase of EHT, respectively (Lancrin et al., 2012; Thambyrajah et al., 2016). Noteworthy, induction of *Runx1* alone without HOXB4 led to a transcriptional repression of the aforementioned hemato-endothelial genes, likely mediated by RUNX1 itself or GFI1 (Lancrin et al., 2012). Taken together, these results prove that the endothelial structures promoted by HOXB4 are indeed hemogenic.

HOXB4 Primes Hemangioblast Progeny toward the Hemogenic Endothelium

Because the number of HE colony-forming cells was increased by HOXB4, we asked whether it expands its upstream progenitor, the hemangioblast (Lancrin et al., 2009). To determine its frequencies, we performed blast colony-forming assays (Choi et al., 1998). As the frequency of $FLK\text{-}1^+$ hemangioblasts (blast colony-forming cells [BL-CFCs]) was highest around day 3.5 of EB development, we isolated $FLK\text{-}1^+$ iRunx cells at that time point and performed blast colony-forming assays with or without HOXB4 expressed constitutively (HOX^{const}) or in an inducible form, HOX^{ERT} (4-hydroxytamoxifen [Tam]-inducible HOXB4-ERT2) (Figure 3A). Two morphologically distinct types of colonies can be detected in this assay, smooth colonies and blast colonies (Lancrin et al., 2009). However, the average numbers of both types of colonies did not significantly change by ectopic HOXB4 expression. The colony frequencies were all at approximately 1%, which is the commonly reported range (Figures 3B and 3D) (Faloon et al., 2000). Thus, HOXB4 did not promote the formation of BL-CFCs. We therefore asked whether HOXB4 alters their fate as an explanation for the observed increase in the number of HE cells. For this purpose, we evaluated the developmental fate of pooled colonies by subjecting those cells into an angiogenic tube formation assay in Matrigel (Arnaoutova and Kleinman, 2010). While control iRunx cells and non-activated $HOXB4^{ERT}$ cells (without Tam) formed meshworks with cords of tubules in Matrigel, cells expressing HOXB4 formed a morphologically distinct mesh of flattened cells without a tubular

(B) The observed endothelial colonies expressed VE-cadherin, CD31, and were capable of acetylated low-density lipoprotein (LDL) (DilAcLDL) uptake. Scale bars, 100 μm.

(C) The number of endothelial $CD31^+$ and $DilAcLDL^+$ colonies strongly increased when HOXB4 was ectopically expressed. Average colony numbers per 10^5 seeded cells are represented as columns, error bars represent SD of n = 3 independent experiments.

(D) iRunx-ESCs with and without a 4-hydroxytamoxifen (Tam) inducible form of HOXB4 (vector FMEV-tdTomato-2A-$HOXB4^{ERT}$) were differentiated as EBs for 6 days, dissociated, and co-cultured on OP9 stroma cells for further 4 days without *Runx1* induction (no addition of doxycycline); n = 9 and 4 independent experiments for controls, n = 7 for HOXB4. Without HOXB4 induction, the number of HE colonies per 10^5 seeded EB cells was comparable with unmanipulated controls. When HOXB4 was induced throughout differentiation, the number of HE colonies increased approximately 30-fold ($p < 10^{-4}$). The p values were calculated using the two-sided, unpaired Student's t test with a significance level defined as 0.05.

(E) Flow cytometric analysis showing the proportion of $CD41^+$ and $CD45^+$ cells in OP9 co-cultures after 5 and 12 days. Dissociated iRunx EBd6 were co-cultured on OP9 cells with or without addition of doxycycline (0.1 μg/mL) to induce *Runx1* expression and with or without addition of 100 nM Tam for induction of $HOXB4^{ERT}$ (FMEV-tdTomato-2A-$HOXB4^{ERT}$). Induction of *Runx1* and $HOXB4^{ERT}$ started from day 3 of EB development on until day 5 of OP9 co-culture. Cells were harvested after 5 or 12 days of OP9 co-culture, and the proportion of CD41- and CD45-expressing cells determined by flow cytometry. OP9 cells were removed with an anti-CD140b antibody.

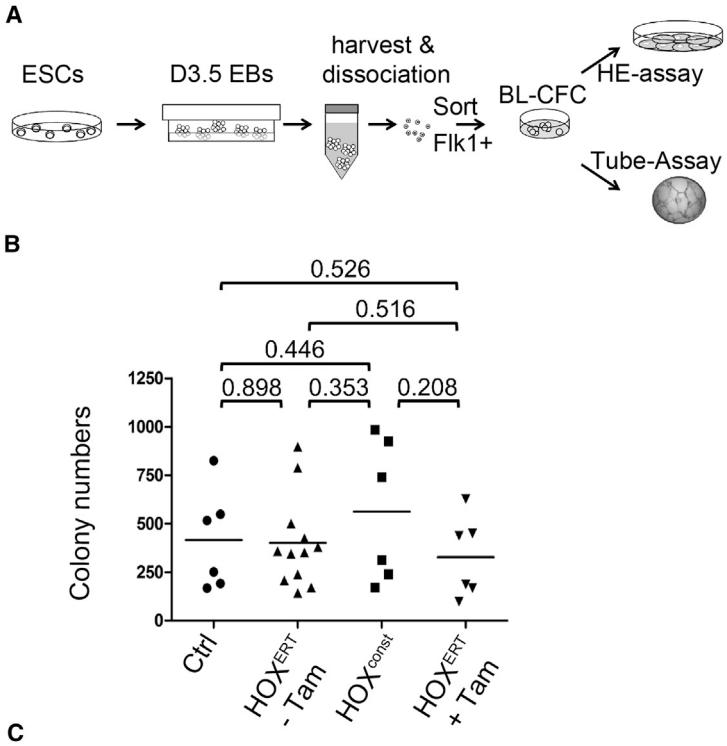

Figure 3. HOXB4 Does Not Alter Blast Colony-Forming Cell (Hemangioblast) Frequencies

(A) Depicted is an overview of FLK-1^{+} hemangioblast frequency determination, subsequent HE quantitation, and evaluation of tube formation propensities. iRunx cells were differentiated as EBs for 3.5 days, FLK-1^{+} cells with and without ectopically expressed HOXB4 were sorted, and 50,000 cells each subjected to blast colony-forming assays to retrospectively quantify the number of hemangioblasts 4 days later. All colonies were harvested, dissociated, and 50,000 cells each placed onto OP9 stroma cells to determine the number of HE colony-forming progenitors 3 days later. A total of 40,000 cells each were placed into a Matrigel-based tube formation assays. All assays were performed at least in triplicate, without *Runx1* induction.

(B) Ectopic HOXB4 expression did not significantly alter the total number of colonies. For statistical analysis, p values were calculated based on the two-sided, unpaired Student's t test, n = 6–12; the significance level was defined as $p < 0.05$. The individual colony numbers are shown as symbols, the arithmetic means depicted as lines.

(C) HOXB4 altered the ability of blast colony cells to form tubes. Instead of the small, thin tubular network observed in the controls (Ctrl and HOXB4^{ERT} without Tam), flat, adherent structures were formed with differing morphologies. The mid-panels show magnifications of the areas indicated in the left pictures. Scale bars, 50 μm.

(D and E) Frequencies of BL-CFCs (arithmetic means, as described in B) (D) and of HE colonies (arithmetic means of n = 3 independent replicates) without HOXB4 induction (HOXB4^{ERT} no Tam) or with constitutively expressed (HOXB4 const) or induced HOXB4 (HOXB4^{ERT} + Tam) (E).

D

Blast Colonies	control	HOX^{ERT} no TAM	HOXB4^{const}	HOX^{ERT} + TAM
average per 50,000 Flk1^{+} cells	417	400	562	327
frequency	8.3/1000	8/1000	11.2/1000	6.5/1000

E

Hemogenic Endothelium	control	HOX^{ERT} no TAM	HOXB4^{const}	HOX^{ERT} + TAM
number of sheets per 50,000 blast colony cells	29	26	> 3,600	> 2,100
frequency	0.6/1000	0.5/1000	70/1000	42/1000

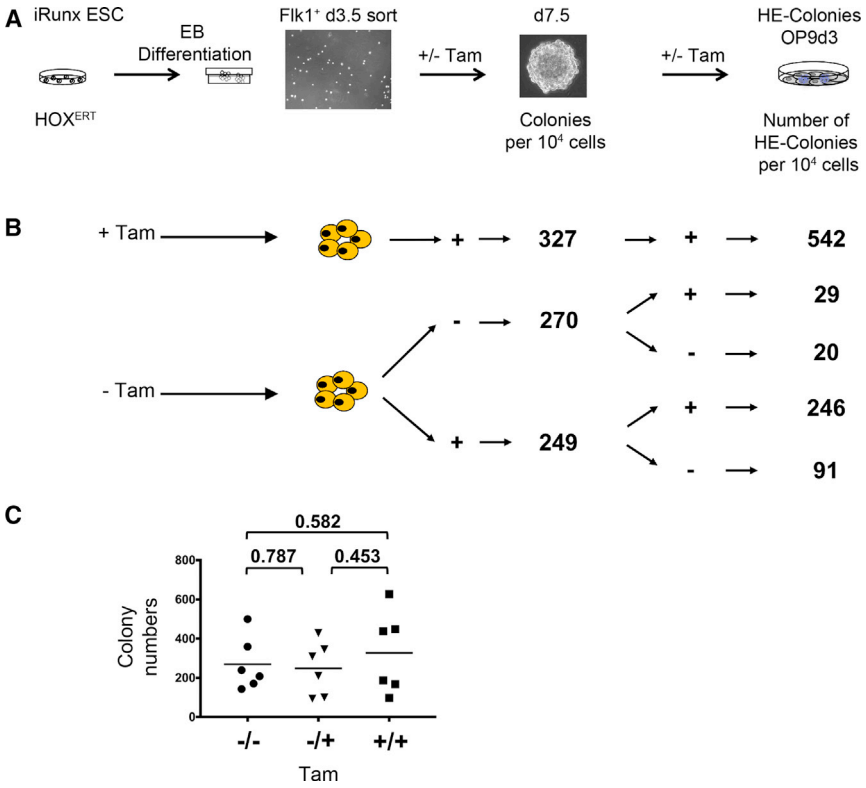

Figure 4. The Progeny of Hemangioblasts Is the Prime Target of HOXB4 Activity

(A) Ectopic HOXB4 activity was induced by addition of Tam at the indicated stages of iRunx-ESC differentiation. BL-CFC assays were performed with 10,000 FLK-1$^+$ iRunx EBd3.5 cells each, +/− Tam.

(B) The total number of colonies was counted 4 days later, the average numbers of n = 3 independent experiments are indicated. +,+,+, Tam (HOXB4) was continuously present; −,−,−, without Tam (no HOXB4 induction); −/−/+, HOXB4 was first induced after dissociation of colonies; −/+/+, HOXB4 was first induced in EBd3.5 FLK-1-sorted cells; −/+/−, HOXB4 was only transiently induced during blast colony formation by FLK-1$^+$ hemangioblasts.

(C) Individual colony numbers and arithmetic means (bars): −/−, no Tam; −/+, induction of HOXB4 in FLK-1-sorted cells; +/+, continuously induced HOXB4. For statistical analysis, an unpaired, two-sided t test with Welch's correction (n = 6) was performed. The p values of individual comparisons are indicated with a significance level defined as $p < 0.05$. To evaluate HE formation, 10,000 cells of pooled, dissociated colonies were placed onto OP9 stroma cells +/− Tam. The numbers of HE colonies grown on OP9 cells after 3 days are shown.

network (Figure 3C). An aliquot was also placed onto OP9 cells to quantify HE colonies. The number of HE colonies was again over 100-fold higher when HOXB4 was constitutively expressed or induced (Figure 3E), therefore suggesting that HOXB4 may alter the developmental fate of either hemangioblasts or their progeny contained within the blast/smooth colonies. To examine this more closely, we induced HOXB4^{ERT} either from the beginning of EB differentiation on, or at different time points prior to and after the blast colony-forming stage in differentiating iRunx cells. Again, the numbers of blast and smooth colonies did not change whether or not HOXB4 was induced in FLK-1$^+$ cells (Figures 4A and 4C). When HOXB4 was first induced after their dissociation, the number of HE structures subsequently formed on OP9 stroma did not increase (Figure 4B, −/−/+ Tam). In contrast, when HOXB4 was already induced during the formation of blast/smooth colonies, the number of subsequent HE colonies markedly increased (Figure 4B, −/+/− Tam). Continuous presence throughout blast and HE colony formation even led to a further increase of HE colonies on OP9 cells (Figure 4B, −/+/+ Tam). These results indicate that HOXB4 primarily acts during the blast culture phase, in cells downstream of the hemangioblast, which may present immediate colony-forming precursors of the HE.

HOXB4 Induces Hemogenic Endothelial Cells without Affecting Endothelial Cell Development

Fate mapping experiments in embryos have suggested that hematopoietic and endothelial cells specify independently from each other or, alternatively, separate early during development (Padron-Barthe et al., 2014; Ueno and Weissman, 2006). Both populations are contained within an FLK-1$^+$PDGFRα^- population, *in vivo* and *in vitro*, which derives from *Etv2*$^+$(*ER71*)$^+$ mesodermal progenitors (Kataoka et al., 1997; Liu et al., 2012; Sakurai et al., 2006; Schatteman et al., 1992; Wareing et al., 2012). To test whether HOXB4 re-specifies endothelial cells toward the hematopoietic fate during early *Runx1*-independent stages, we deposited single FLK-1$^+$ PDGFRα^- cells from d4 iRunx EBs on OP9 stromal cells and determined the frequencies of circular, cobblestone-like CD31$^+$ (Pecam1) hemogenic and of elongated endothelial colonies formed after further 4 days. We then asked whether the frequencies change after induction of HOXB4 (Figure 5A). Irrespective if HOXB4 was induced

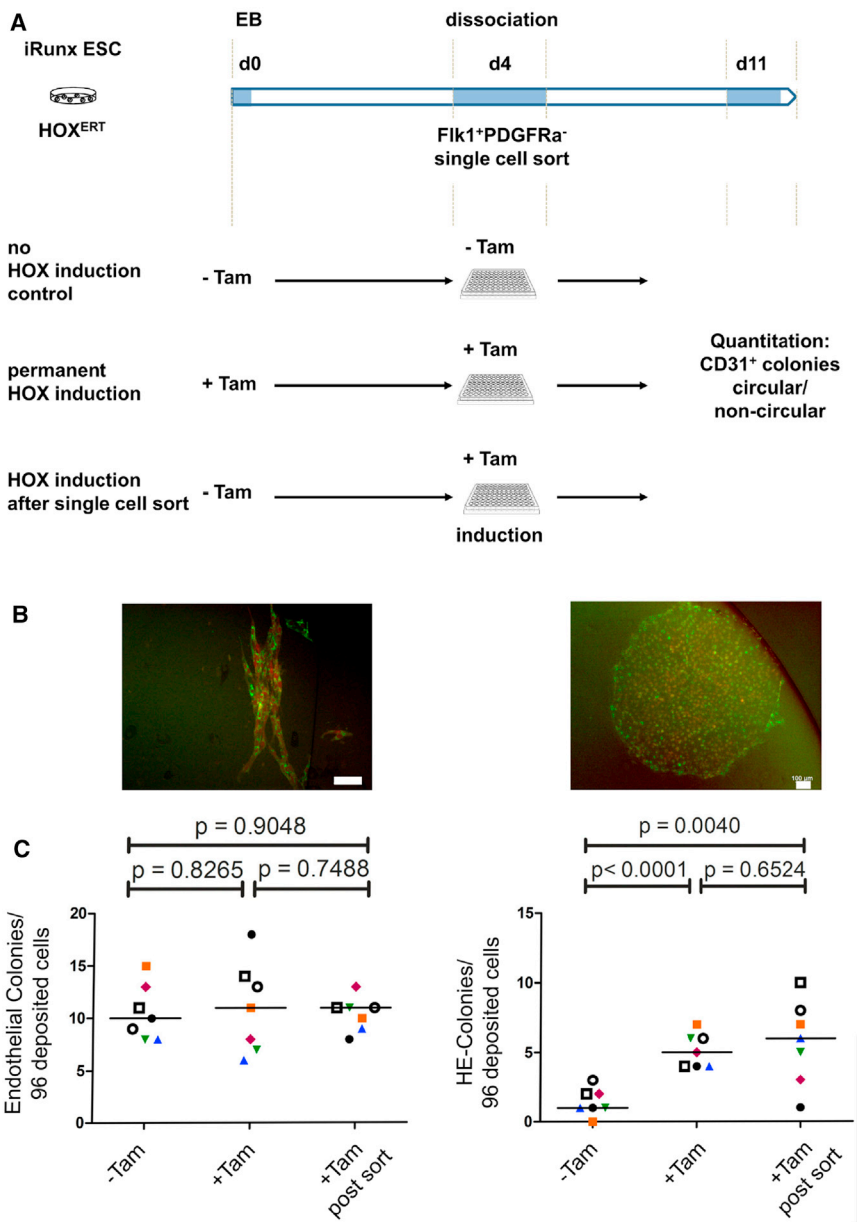

Figure 5. HOXB4 Does Not Re-specify Endothelial Cells to a Hematopoietic Fate

(A) iRunx ESCs expressing tamoxifen-inducible HOXB4 (tdTomato-2A-HOXB4^{ERT}) were differentiated as EBs for 4 days, dissociated, and single FLK-1^{+}PDGFRα^{-} cells deposited and co-cultured with OP9 cells in 96-well plates. After a further 4 days, CD31^{+} tdTomato/HOXB4^{+} colonies were counted and qualified either as "endothelial colony" or "HE colony."

(B) Typical colony morphologies. Scale bars, 100 μm.

(C) Quantification of endothelial and HE colonies formed by single deposited cells +/− HOXB4 induction. –Tam, without HOXB4^{ERT} induction; +Tam, permanent induction of HOXB4^{ERT}. +Tam post sort, induction after single-cell deposition. The p values as calculated by Student's t test, paired and two-sided, with a significance level defined as 0.05, are indicated above. Forms and colors indicate endothelial and HE colonies grown on the same 96-well plate.

or not, the frequencies of CD31^{+} endothelial, strand-like colonies were unchanged (Figures 5B and 5C). In contrast, when HOXB4 was induced, either throughout differentiation or immediately after single-cell deposition, the number of circular HE colonies significantly increased compared with the non-induced control. Possible explanations are that HOXB4 either mediated enhanced proliferation of HE precursors or, alternatively, protected them from apoptosis. To test these possibilities we induced HOXB4 in FLK-1^{+} cells purified from day 3.5 EBs and subjected them to blast culture conditions. After 24 and 48 hr, we either pulse-labeled replicating DNA with EdU for 2.5 hr or determined the proportion of apoptotic cells by annexin V and DAPI staining. Neither proliferation nor apoptosis of FLK-1^{+} progenitor cells was altered after induction of HOXB4 (Figure S4).

Taken together, the results indicate the following: (1) HOXB4 does not re-specify FLK-1^{+}PDGFRα^{-} endothelial cells toward a hematopoietic fate because, otherwise, the endothelial colony numbers would have decreased after HOXB4 induction. (2) Induction of HOXB4 in single mesodermal FLK-1^{+} cells does not enhance their proliferative activity or inhibit apoptosis, but instead activates an endogenous program allowing them to form HE colonies and realize their hematopoietic potential as soon as *Runx1* is switched on.

The Transcriptional Signature of ESC-Derived Mesodermal Cells Ectopically Expressing HOXB4 Indicates the Acquisition of a Hemogenic Endothelial Fate

As HOXB4 does not appear to re-specify endothelial cells but, instead, activates a hematogenic program in single FLK-1$^+$PDGFRα^- cells, we asked how HOXB4 rewires the transcriptional regulatory circuits during a RUNX1-independent stage of hematopoietic development. To answer that question, we compared the transcriptional profiles of FLK-1$^+$PDGFRα^- cell populations purified from iRunx day 4 EBs with and without ectopic HOXB4 expression. Among mRNAs that were upregulated (321), we found transcripts that are necessary for hematopoietic specification, such as *Scl/Tal1*, *Gata2*, *Fli1*, *Tie2*, *Erg*, *Kit*, *Egfl7*, *Lyl1*, *Myb*, *Sox7*, or *Hhex*, as well as transcripts encoding hemato-endothelial surface molecules *Cdh5* (VE-cadherin), *CD34*, or *CD109* (Figures 6A and 6B; Table S1). Notably, most of the so-called heptad TF-encoding genes, which co-operate to promote hematopoiesis, were significantly upregulated in the HOXB4-iRunx cells (*Tal1, Lyl1, Fli1, Gata2, Erg*, and *Lmo2*, except *Runx1*) (Figure 6B) (Wilson et al., 2010). Downregulated mRNAs (178) comprised transcripts that encode proteins associated with mesodermal and cardiovascular development, such as *Hand1*, *Mixl1*, *Gata4*, *Foxf1*, *Foxh1*, *Lef1*, *Etv2*, *Fgf15*, or *Tgfb2* (Figure 6A, lower panel; Table S1).

To test if these cells displayed a gene expression signature corresponding to a hemato-endothelial precursor, *in vivo*, we first asked which mesodermal cell type of the gastrulating embryo the iRunx-derived cells +/− HOXB4 most closely relate to molecularly (Scialdone et al., 2016). Gene set enrichment analysis (GSEA) (Subramanian et al., 2005) uncovered that FLK-1$^+$PDGFRα^-RUNX1$^-$ cells without ectopic HOXB4 most closely resembled a transcriptional signature of early mesodermal progenitors of the neural plate stage (E7.5). In contrast, cells expressing activated HOXB4 displayed a significant enrichment of genes expressed in hemato-endothelial progenitors of the head-fold stage (E7.75) (Figure 6C; Table S2). To further refine the analysis we asked how closely these iRunx-derived cells resembled hemato-endothelial cells of E8.5 transgenic *Runx1*-reporter ("+23GFP") mouse embryos (Swiers et al., 2013). GSEA indicated a closer relationship of FLK-1$^+$PDGFRα^- EBd4 iRunx cells to 23GFP$^-$/RUNX1$^-$ hemato-endothelial cells then to GFP$^+$/RUNX1$^+$ HE cells (Figure 6C; Table S2). This was not surprising, as *Runx1* was not induced in the iRunx cells. However, the results point out that ectopic HOXB4 cannot initiate those transcriptional programs critical for subsequent steps of hematopoietic development without the activity of RUNX1. We finally asked whether the transcriptome of HOXB4 cells rather displayed an endothelial or HE signature using gene sets from dorsal aorta cells of E10 transgenic *Sca1*-reporter (*Ly6aGFP*) mice (Solaimani Kartalaei et al., 2015). Although *Runx1* was not induced in the iRunx cells, GSEA clearly indicated similarity of HOXB4-expressing EBd4 iRunx cells to dorsal aorta-resident HE cells (Figure 6C; Table S2).

DISCUSSION

Two main concepts exist with regard to how the HE is formed during embryonic development. One is based on a dichotomic model in which binary fate decisions happen during cell divisions throughout development. The FLK-1$^+$ hemangioblast, a progenitor cell thought to generate all vascular endothelial and hematopoietic cells fits to the idea (Choi et al., 1998; Lancrin et al., 2009; Nishikawa, 2012). The other possibility is that endothelial and hematopoietic lineages separate during an earlier developmental stage and develop independently of each other. This concept is supported by cell tracing analysis in embryos (Padron-Barthe et al., 2014; Ueno and Weissman, 2006). In that case, the hemangioblast could present a specialized, transiently existing endothelial cell with the competence to acquire a hematopoietic fate upon environmental cues mediated, for example, by Notch or Wnt signaling (Richard et al., 2013).

When ectopically expressing HOXB4 in differentiating iRunx cells, we did not observe a significant change in the numbers of blast colony-forming hemangioblasts. However, when we tested the developmental competence of the progeny of these cells to form HE colonies, we observed a strong increase in their numbers when HOXB4 was induced during blast colony formation of FLK-1$^+$ cells. Hence, HOXB4 appeared to promote the hematopoietic fate in HE precursors downstream of the hemangioblast. Supporting this idea, deposition of single FLK-1$^+$PDGFRα^- cells and induction of HOXB4 significantly promoted the formation of circular, cobblestone-like HE colonies, which underwent EHT after induction of *Runx1*. Interestingly, the number of cord-formed endothelial colonies was unchanged, irrespective if HOXB4 was activated or not. If HOXB4 would directly act as a fate determinant in hemangioblasts, the increase of HE colonies must have been accompanied by a concomitant decrease in the number of endothelial colonies. However, that was not the case, thus supporting the interpretation that HOXB4 acts after the hemangioblast stage in precursors of the HE.

Genome-wide transcriptional profiling revealed that HOXB4 induced the expression of a plethora of genes essential for hematopoiesis. Particularly, most of the heptad-TF genes were upregulated during early differentiation of iRunx-ESCs (except *Runx1*). The encoded TFs are known

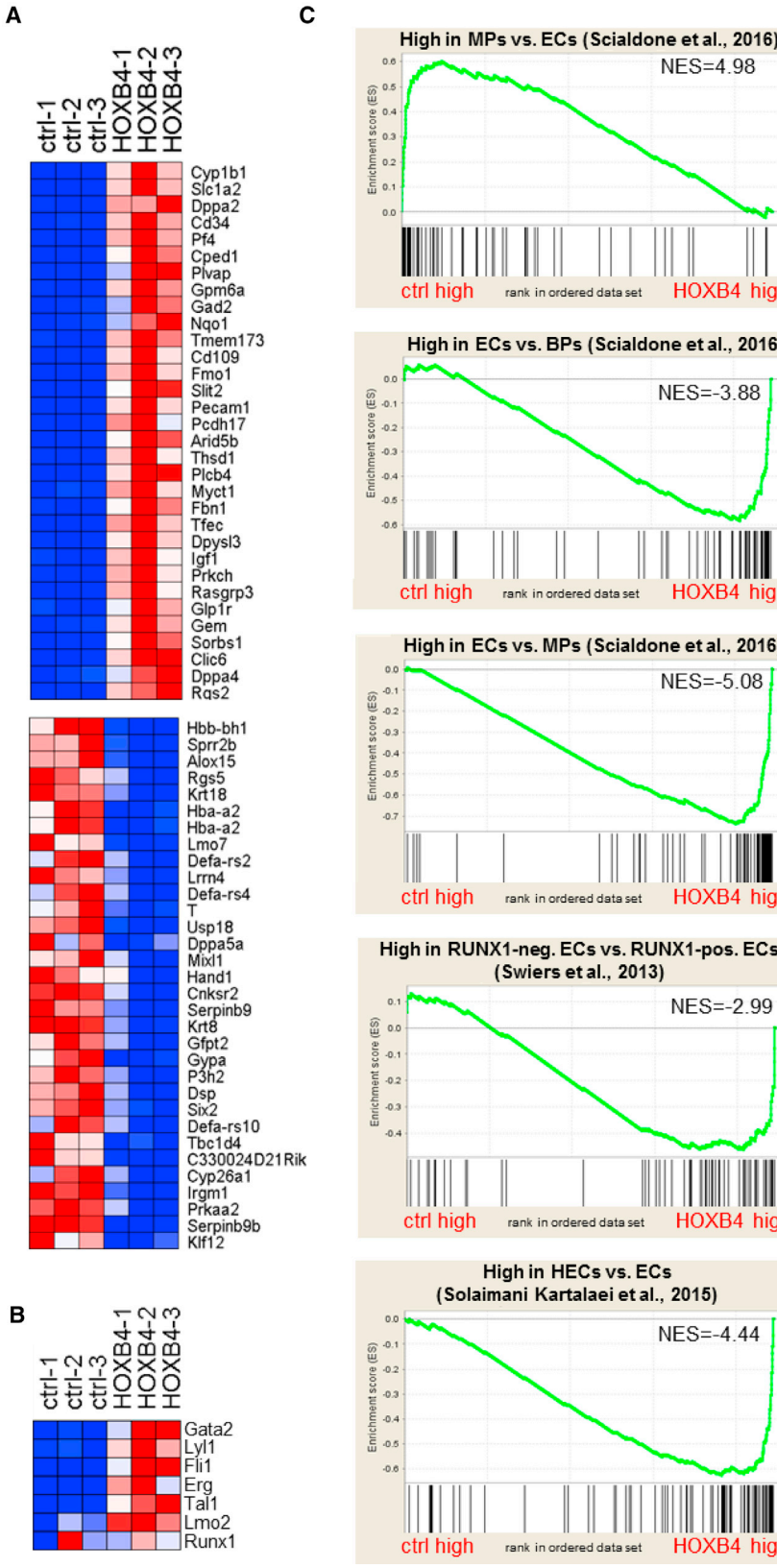

Figure 6. Gene Expression Profiling of FLK-1^{+}PDGFRα^{-} Cells

(A) Heatmap showing the top 32 genes (fold-change ranked) either up- or downregulated in FLK-1^{+}PDGFRα^{-} cell populations from iRunx day 4 EBs without (ctrl) or with ectopically expressed HOXB4. Genes were considered differentially expressed if they met two criteria: q $\leq$ 0.2 and fold-change $\geq$ 2.0 (499 genes) (for full list see Table S1).

(B) Heatmap for the expression of heptad transcription factors.

(C) GSEA using gene sets specific for mesodermal progenitors ([MPs] top panel) compared with endothelial cells (ECs), ECs compared with blood progenitors ([BPs] second panel) and endothelial cells compared with mesodermal progenitors (third panel) (Scialdone et al., 2016); E8.5 RUNX^{-} endothelial cells (RUNX1-neg. ECs) compared with RUNX1^{+} endothelial cells (RUNX1-pos. ECs, fourth panel) (Swiers et al., 2013) and E10 hemogenic endothelial cells (HECs) compared with endothelial cells (ECs, fifth panel) (Solaimani Kartalaei et al., 2015). Genes were drawn according to their rank from left (high expression in control) to right (high expression in HOXB4-expressing cells) and gene sets plotted on top with each black bar representing a gene. The enrichment score is plotted in on the vertical axis.

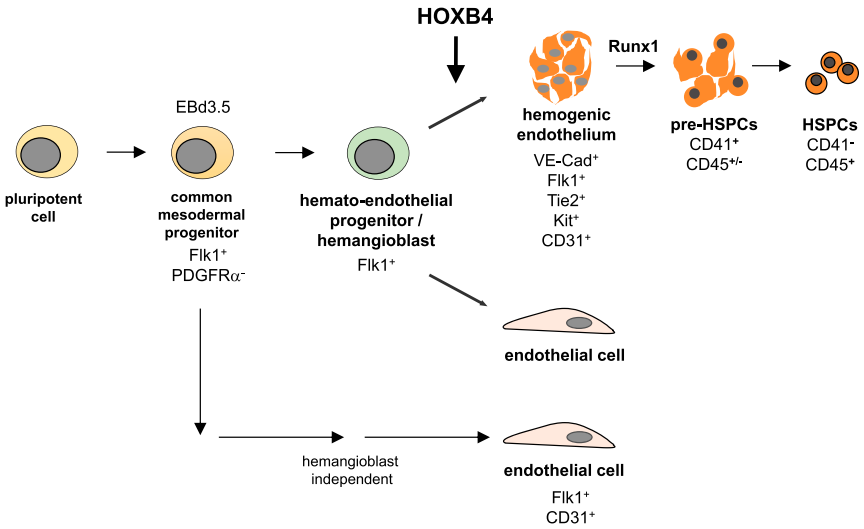

Figure 7. Model of HOXB4 Activity during Pluripotent Stem Cell Differentiation

During mouse ESC differentiation, HOXB4 appears to promote hematopoietic commitment after the hemangioblast stage in VE-Cad$^+$FLK-1$^+$TIE2$^+$KIT$^+$CD31$^+$ precursors of HE cells by upregulating the expression of key hematopoietic transcription factors, in a RUNX1-independent fashion. Importantly, our results indicate that this does not happen at the expense of endothelial cells. These results are also compatible with the notion that (at least a part of) endothelial cells develop hemangioblast-independently (Padron-Barthe et al., 2014; Ueno and Weissman, 2006).

to co-operatively regulate genes essential for hematopoietic development (Wilson et al., 2010). Importantly, HOXB4 has previously been shown to physically bind upstream of all of these seven genes (Fan et al., 2012). For example, it directly binds to the conserved +85 kb enhancer element of *Erg* (Moignard et al., 2015; Wilson et al., 2009), which is also bound by most of the heptad TFs (Schutte et al., 2016). Furthermore, HOXB4 binds to DNA in close proximity to the TFs FLI-1, MEIS1, RUNX1, and SCL (Fan et al., 2012), strongly implying its participation in a TF complex regulating common hematopoietic target genes. GSEA with gene sets derived from hematopoietic tissues that had been isolated by different means and different stages (E7.5–E10) of embryonic development (Scialdone et al., 2016; Solaimani Kartalaei et al., 2015; Swiers et al., 2013) indicated that HOXB4$^+$FLK-1$^+$PDGFRα^- cells most closely resembled HE cells of the dorsal aorta in E10 embryos. Given that endogenous mouse *HoxB4* is also expressed at low levels around this stage, *in vivo* (Moignard et al., 2015), ectopic overexpression of human HOXB4 in differentiating ESCs may simply represent a fortification of embryonic hematopoiesis.

Our results with HOXB4 may be paradigmatic for the activities of all HOX4 paralogs, as ectopic expression of the other orthologs HOXA4, C4, and D4 similarly enhanced hematopoietic development of differentiating ESCs (Iacovino et al., 2009). HOXB4 directly binds to a region between the proximal (P2) and distal (P1) promoters of *Runx1*, which correlates with demethylation and activation of the P1 promoter (Webber et al., 2013). This may probably explain our observation of *Runx1* upregulation in a small subpopulation of ESC-derived HE cells, *in vitro* (Teichweyde et al., 2017). How homeotic selector proteins mechanistically influence cell fate decisions during development is not well understood yet. It appears that their activities as activators or repressors of transcription depend on their expression levels, the cell type they are expressed in, and probably also the microenvironment of the cells (Klump et al., 2005; Pilat et al., 2005; Schiedlmeier et al., 2003, 2007; Will et al., 2006). It could be envisioned that these master switches of development integrate signaling events allowing for the realization of certain genetic programs by epigenetically promoting enhancer activation or decommission.

In the present work we have shown that HOXB4 first unfolds its hematopoiesis-promoting activity in HE precursors (summarized in Figure 7). By inducing a hematopoietic program in those cells, HOXB4 promotes the acquisition of an HE identity and, thus, enforces early hematopoietic development. It remains to be shown if this also holds true for differentiating human pluripotent stem cells, as this would open the possibility to enhance the generation of patient-specific HSPCs. In fact, a recent report strongly suggests that ectopic HOXB4 expression also promotes hematopoietic development of human ESCs (Jackson et al., 2016), therefore supporting the idea of what is true for mouse hematopoietic development also holds true for humans.

EXPERIMENTAL PROCEDURES

For production of retroviral vectors, ESC culture, hematopoietic differentiation, mouse transplantation, colony-forming assays, gene expression analysis, and time-lapse microscopy, see Supplemental Information. All animal experiments were approved by the Landesamt für Natur, Umwelt und Verbraucherschutz Nordrhein-Westfalen (LANUV) (reference number 84-02.04.2013.A350) and were performed according to official guidelines and regulations.

Blast Colony-Forming Assays

Blast colony assays were performed as described (Kennedy and Keller, 2003). In brief, 5×10^5 ESCs were differentiated as EBs for 3.5 days, dissociated and FLK-1$^+$ cells sorted by flow cytometry (FACSAria III, BD Biosciences). Cells were subsequently cultured at a concentration of 5×10^4 cells/mL for 4–5 days in IMDM containing 10% (v/v) fetal calf serum (GE Healthcare), 2 mM L-glutamine, 20% (v/v) D4T conditioned medium, 1% (v/v) penicillin/streptomycin, 4.5×10^{-4} M MTG, 25 ng/mL ascorbic acid, 300 μg/mL holotransferrin (Sigma-Aldrich), 10 ng/mL rhIL-6, 5 ng/mL rhVEGF, 25% methylcellulose solution, under hypoxic conditions (3% O_2) at 37°C in a H_2O saturated atmosphere.

Tube Formation Assay

To assess the angiogenic activity of cells contained within blast colonies, 4×10^4 cells were cultured in μ-Slide Angiogenesis chambers (ibidi) filled with 10 μL Matrigel matrix (Corning Life Sciences) for 19 hr at 37°C in H_2O saturated atmosphere, 3% O_2, 5% CO_2.

Flow Cytometry Analysis and Cell Sorting

Differentiating ESCs, bone marrow and peripheral blood of transplanted mice were analyzed by flow cytometry using fluorochrome-conjugated monoclonal antibodies. Details regarding employed antibodies (specificities, manufacturer, catalog numbers) are listed in the Supplemental Experimental Procedures section.

For FACS analysis, dead cells were excluded by DAPI staining. Gates were set based on control samples stained according to the Fluorescence Minus One method. Flow cytometry measurements and single-cell sorting were performed on a FACSAria III instrument (BD Biosciences) using FACSDiva software, datasets were analyzed using FlowJo software (Tree Star).

Magnet-Activated Cell Sorting

For removal of stroma cells, magnet-activated cell sorting (MACS) technology was used (Miltenyi). Harvested cells were incubated either with Feeder Removal MicroBeads (for removal of CF1-MEFs) or with an anti-CD140b PE-labeled mAB (OP9) and anti-PE microbeads, and subsequently depleted with MACS LS Columns, according to the manufacturer's recommendations.

Transcriptome Analysis

iRunx EBd4 were dissociated and FLK-1$^+$PDFGRα$^-$ cells with or without retroviral expression of tdTomato/HOXB4 were sorted by FACS. Total RNA was extracted using TRIzol and subsequently purified with RNeasy columns (QIAGEN). Each sample (500 ng) was converted into fragmented, biotinylated cDNA hybridized to a microarray chip (Clariome D MTA 1.0) and fluorescently labeled according to the standard protocol (Affymetrix, Santa Clara, CA). Raw data were processed in Expression Console (Affymetrix) using RMA normalization and expression values calculated for each Refseq-annotated gene (23,781 total). The expression data were processed in Gene Pattern (Broad Institute, Cambridge, MA). Non-expressed genes were filtered out, and the resulting expression matrix was analyzed with the comparative marker module. GSEA (Broad Institute) was performed as described previously (Subramanian et al., 2005). Genes sets (Table S2) were derived from associated publications as indicated in the text.

Statistical Analysis

Significance testing of differences between mean values was performed by calculating p values using the two-sided unpaired, Student's t test. Significance levels were defined as $p < 0.05$. For all calculations, GraphPad Prism6 software (GraphPad, CA, USA) was used.

ACCESSION NUMBERS

The accession number for the microarray data reported in this paper is GEO: GSE103627.

SUPPLEMENTAL INFORMATION

Supplemental Information includes Supplemental Experimental Procedures, four figures, two tables, and two movies and can be found with this article online at https://doi.org/10.1016/j.stemcr.2018.01.009.

AUTHOR CONTRIBUTIONS

Conceptualization, H.K.; Methodology, N.T., L.K., S.H., S.C., G.L., V.K., and H.K.; Formal Analysis, N.T., L.K., and S.H.; Investigation, N.T. and L.K.; Resources, G.L. and V.K.; Data Curation, N.T., L.K., S.H., and H.K.; Writing – Original Draft, H.K.; Writing – Review & Editing, N.T., L.K., S.H., S.C., G.L., V.K., P.A.H., and H.K.; Visualization, N.T., L.K., S.H., and H.K.; Supervision, H.K.; Project Administration, H.K.; Funding Acquisition, H.K. and P.A.H.

ACKNOWLEDGMENTS

We wish to thank Jörg Fehling (Institute for Immunology, University of Ulm, Germany) for providing the GFP-Bry mouse reporter ESCs, Samantha Langer and Martina Cremanns for their help during mouse transplantation experiments, and Antje Kleinbielen and Susanne Skibbe for excellent technical support. This work was supported by the Deutsche Forschungsgemeinschaft (DFG grants KL1311/5-1 and KL1311/8-1) and the Else Kröner-Fresenius-Stiftung (support of *ELAN* graduate program student L.K.). Research in G.L.'s laboratory is supported by the Biotechnology and Biological Sciences Research Council (BB/I001794/1), Bloodwise (12037), the European Union's Horizon 2020 (GA6586250), and Cancer Research UK (C5759/A20971). Research in V.K.'s laboratory is supported by the Medical Research Council (MR/P000673/1) and the Biotechnology and Biological Sciences Research Council (BB/I001794/1).

Received: October 4, 2016
Revised: January 15, 2018
Accepted: January 16, 2018
Published: February 15, 2018

REFERENCES

Abate-Shen, C. (2002). Deregulated homeobox gene expression in cancer: cause or consequence? Nat. Rev. Cancer *2*, 777–785.

Arnaoutova, I., and Kleinman, H.K. (2010). In vitro angiogenesis: endothelial cell tube formation on gelled basement membrane extract. Nat. Protoc. *5*, 628–635.

Azcoitia, V., Aracil, M., Martínez, A.C., and Torres, M. (2005). The homeodomain protein Meis1 is essential for definitive hematopoiesis and vascular patterning in the mouse embryo. Dev. Biol. *280*, 307–320.

Bertrand, J.Y., Chi, N.C., Santoso, B., Teng, S., Stainier, D.Y., and Traver, D. (2010). Haematopoietic stem cells derive directly from aortic endothelium during development. Nature *464*, 108–111.

Bloor, A.J., Sanchez, M.J., Green, A.R., and Gottgens, B. (2002). The role of the stem cell leukemia (SCL) gene in hematopoietic and endothelial lineage specification. J. Hematother. Stem Cell Res. *11*, 195–206.

Chan, K.M., Bonde, S., Klump, H., and Zavazava, N. (2008). Hematopoiesis and immunity of HOXB4-transduced embryonic stem cell-derived hematopoietic progenitor cells. Blood *111*, 2953–2961.

Choi, K., Kennedy, M., Kazarov, A., Papadimitriou, J.C., and Keller, G. (1998). A common precursor for hematopoietic and endothelial cells. Development *125*, 725–732.

Eilken, H.M., Nishikawa, S., and Schroeder, T. (2009). Continuous single-cell imaging of blood generation from haemogenic endothelium. Nature *457*, 896–900.

Ema, M., Faloon, P., Zhang, W.J., Hirashima, M., Reid, T., Stanford, W.L., Orkin, S., Choi, K., and Rossant, J. (2003). Combinatorial effects of Flk1 and Tal1 on vascular and hematopoietic development in the mouse. Genes Dev. *17*, 380–393.

Faloon, P., Arentson, E., Kazarov, A., Deng, C.X., Porcher, C., Orkin, S., and Choi, K. (2000). Basic fibroblast growth factor positively regulates hematopoietic development. Development *127*, 1931–1941.

Fan, R., Bonde, S., Gao, P., Sotomayor, B., Chen, C., Mouw, T., Zavazava, N., and Tan, K. (2012). Dynamic HoxB4-regulatory network during embryonic stem cell differentiation to hematopoietic cells. Blood *119*, e139–147.

Fehling, H.J., Lacaud, G., Kubo, A., Kennedy, M., Robertson, S., Keller, G., and Kouskoff, V. (2003). Tracking mesoderm induction and its specification to the hemangioblast during embryonic stem cell differentiation. Development *130*, 4217–4227.

Gritz, E., and Hirschi, K.K. (2016). Specification and function of hemogenic endothelium during embryogenesis. Cell. Mol. Life Sci. *73*, 1547–1567.

Iacovino, M., Hernandez, C., Xu, Z., Bajwa, G., Prather, M., and Kyba, M. (2009). A conserved role for Hox paralog group 4 in regulation of hematopoietic progenitors. Stem Cells Dev. *18*, 783–792.

Iwasaki, H., Somoza, C., Shigematsu, H., Duprez, E.A., Iwasaki-Arai, J., Mizuno, S., Arinobu, Y., Geary, K., Zhang, P., Dayaram, T., et al. (2005). Distinctive and indispensable roles of PU.1 in maintenance of hematopoietic stem cells and their differentiation. Blood *106*, 1590–1600.

Jackson, M., Axton, R.A., Taylor, A.H., Wilson, J.A., Gordon-Keylock, S.A., Kokkaliaris, K.D., Brickman, J.M., Schulz, H., Hummel, O., Hubner, N., et al. (2012). HOXB4 can enhance the differentiation of embryonic stem cells by modulating the hematopoietic niche. Stem Cells *30*, 150–160.

Jackson, M., Ma, R., Taylor, A.H., Axton, R.A., Easterbrook, J., Kydonaki, M., Olivier, E., Marenah, L., Stanley, E.G., Elefanty, A.G., et al. (2016). Enforced expression of HOXB4 in human embryonic stem cells enhances the production of hematopoietic progenitors but has no effect on the maturation of red blood cells. Stem Cells Transl. Med. *5*, 981–990.

Jaffredo, T., Gautier, R., Eichmann, A., and Dieterlen-Lievre, F. (1998). Intraaortic hemopoietic cells are derived from endothelial cells during ontogeny. Development *125*, 4575–4583.

Kataoka, H., Hayashi, M., Nakagawa, R., Tanaka, Y., Izumi, N., Nishikawa, S., Jakt, M.L., Tarui, H., and Nishikawa, S. (2011). Etv2/ER71 induces vascular mesoderm from Flk1+PDGFRalpha+ primitive mesoderm. Blood *118*, 6975–6986.

Kataoka, H., Takakura, N., Nishikawa, S., Tsuchida, K., Kodama, H., Kunisada, T., Risau, W., Kita, T., and Nishikawa, S.I. (1997). Expressions of PDGF receptor alpha, c-Kit and Flk1 genes clustering in mouse chromosome 5 define distinct subsets of nascent mesodermal cells. Dev. Growth Differ. *39*, 729–740.

Kennedy, M., Firpo, M., Choi, K., Wall, C., Robertson, S., Kabrun, N., and Keller, G. (1997). A common precursor for primitive erythropoiesis and definitive haematopoiesis. Nature *386*, 488–493.

Kennedy, M., and Keller, G.M. (2003). Hematopoietic commitment of ES cells in culture. Methods Enzymol. *365*, 39–59.

Klump, H., Schiedlmeier, B., and Baum, C. (2005). Control of self-renewal and differentiation of hematopoietic stem cells: HOXB4 on the threshold. Ann. N. Y. Acad. Sci. *1044*, 6–15.

Klump, H., Teichweyde, N., Meyer, C., and Horn, P.A. (2013). Development of patient-specific hematopoietic stem and progenitor cell grafts from pluripotent stem cells, in vitro. Curr. Mol. Med. *13*, 815–820.

Kyba, M., Perlingeiro, R.C., and Daley, G.Q. (2002). HoxB4 confers definitive lymphoid-myeloid engraftment potential on embryonic stem cell and yolk sac hematopoietic progenitors. Cell *109*, 29–37.

Lacaud, G., Gore, L., Kennedy, M., Kouskoff, V., Kingsley, P., Hogan, C., Carlsson, L., Speck, N., Palis, J., and Keller, G. (2002). Runx1 is essential for hematopoietic commitment at the hemangioblast stage of development in vitro. Blood *100*, 458–466.

Lancrin, C., Mazan, M., Stefanska, M., Patel, R., Lichtinger, M., Costa, G., Vargel, O., Wilson, N.K., Moroy, T., Bonifer, C., et al. (2012). GFI1 and GFI1B control the loss of endothelial identity of hemogenic endothelium during hematopoietic commitment. Blood *120*, 314–322.

Lancrin, C., Sroczynska, P., Stephenson, C., Allen, T., Kouskoff, V., and Lacaud, G. (2009). The haemangioblast generates haematopoietic cells through a haemogenic endothelium stage. Nature *457*, 892–895.

Lesinski, D.A., Heinz, N., Pilat-Carotta, S., Rudolph, C., Jacobs, R., Schlegelberger, B., Klump, H., and Schiedlmeier, B. (2012). Serum- and stromal cell-free hypoxic generation of embryonic stem cell-derived hematopoietic cells in vitro, capable of multilineage repopulation of immunocompetent mice. Stem Cells Transl. Med. *1*, 581–591.

Liu, F., Bhang, S.H., Arentson, E., Sawada, A., Kim, C.K., Kang, I., Yu, J., Sakurai, N., Kim, S.H., Yoo, J.J., et al. (2013). Enhanced hemangioblast generation and improved vascular repair and regeneration from embryonic stem cells by defined transcription factors. Stem Cell Reports *1*, 166–182.

Liu, F., Kang, I., Park, C., Chang, L.W., Wang, W., Lee, D., Lim, D.S., Vittet, D., Nerbonne, J.M., and Choi, K. (2012). ER71 specifies Flk-1+ hemangiogenic mesoderm by inhibiting cardiac mesoderm and Wnt signaling. Blood *119*, 3295–3305.

Liu, F., Li, D., Yu, Y.Y., Kang, I., Cha, M.J., Kim, J.Y., Park, C., Watson, D.K., Wang, T., and Choi, K. (2015). Induction of hematopoietic and endothelial cell program orchestrated by ETS transcription factor ER71/ETV2. EMBO Rep. *16*, 654–669.

Lu, Y.F., Cahan, P., Ross, S., Sahalie, J., Sousa, P.M., Hadland, B.K., Cai, W., Serrao, E., Engelman, A.N., Bernstein, I.D., et al. (2016). Engineered murine HSCs reconstitute multi-lineage hematopoiesis and adaptive immunity. Cell Rep. *17*, 3178–3192.

McKinney-Freeman, S.L., Naveiras, O., Yates, F., Loewer, S., Philitas, M., Curran, M., Park, P.J., and Daley, G.Q. (2009). Surface antigen phenotypes of hematopoietic stem cells from embryos and murine embryonic stem cells. Blood *114*, 268–278.

Moignard, V., Woodhouse, S., Haghverdi, L., Lilly, A.J., Tanaka, Y., Wilkinson, A.C., Buettner, F., Macaulay, I.C., Jawaid, W., Diamanti, E., et al. (2015). Decoding the regulatory network of early blood development from single-cell gene expression measurements. Nat. Biotechnol. *33*, 269–276.

Nishikawa, S. (2012). Hemangioblast: an in vitro phantom. Wiley Interdiscip. Rev. Dev. Biol. *1*, 603–608.

Nishikawa, S.I., Nishikawa, S., Hirashima, M., Matsuyoshi, N., and Kodama, H. (1998). Progressive lineage analysis by cell sorting and culture identifies FLK1+VE-cadherin+ cells at a diverging point of endothelial and hemopoietic lineages. Development *125*, 1747–1757.

North, T., Gu, T.L., Stacy, T., Wang, Q., Howard, L., Binder, M., Marin-Padilla, M., and Speck, N.A. (1999). Cbfa2 is required for the formation of intra-aortic hematopoietic clusters. Development *126*, 2563–2575.

Oshima, M., Endoh, M., Endo, T.A., Toyoda, T., Nakajima-Takagi, Y., Sugiyama, F., Koseki, H., Kyba, M., Iwama, A., and Osawa, M. (2011). Genome-wide analysis of target genes regulated by HoxB4 in hematopoietic stem and progenitor cells developing from embryonic stem cells. Blood *117*, e142–e150.

Padron-Barthe, L., Temino, S., Villa del Campo, C., Carramolino, L., Isern, J., and Torres, M. (2014). Clonal analysis identifies hemogenic endothelium as the source of the blood-endothelial common lineage in the mouse embryo. Blood *124*, 2523–2532.

Pearson, S., Cuvertino, S., Fleury, M., Lacaud, G., and Kouskoff, V. (2015). In vivo repopulating activity emerges at the onset of hematopoietic specification during embryonic stem cell differentiation. Stem Cell Reports *4*, 431–444.

Pilat, S., Carotta, S., Schiedlmeier, B., Kamino, K., Mairhofer, A., Will, E., Modlich, U., Steinlein, P., Ostertag, W., Baum, C., et al. (2005). HOXB4 enforces equivalent fates of ES-cell-derived and adult hematopoietic cells. Proc. Natl. Acad. Sci. USA *102*, 12101–12106.

Richard, C., Drevon, C., Canto, P.Y., Villain, G., Bollérot, K., Lempereur, A., Teillet, M.A., Vincent, C., Rosselló Castillo, C., Torres, M., et al. (2013). Endothelio-mesenchymal interaction controls runx1 expression and modulates the notch pathway to initiate aortic hematopoiesis. Dev. Cell *24*, 600–611.

Sakurai, H., Era, T., Jakt, L.M., Okada, M., Nakai, S., Nishikawa, S., and Nishikawa, S. (2006). In vitro modeling of paraxial and lateral mesoderm differentiation reveals early reversibility. Stem Cells *24*, 575–586.

Schatteman, G.C., Morrison-Graham, K., van Koppen, A., Weston, J.A., and Bowen-Pope, D.F. (1992). Regulation and role of PDGF receptor alpha-subunit expression during embryogenesis. Development *115*, 123–131.

Schiedlmeier, B., Klump, H., Will, E., Arman-Kalcek, G., Li, Z., Wang, Z., Rimek, A., Friel, J., Baum, C., and Ostertag, W. (2003). High-level ectopic HOXB4 expression confers a profound in vivo competitive growth advantage on human cord blood CD34+ cells, but impairs lymphomyeloid differentiation. Blood *101*, 1759–1768.

Schiedlmeier, B., Santos, A.C., Ribeiro, A., Moncaut, N., Lesinski, D., Auer, H., Kornacker, K., Ostertag, W., Baum, C., Mallo, M., et al. (2007). HOXB4's road map to stem cell expansion. Proc. Natl. Acad. Sci. USA *104*, 16952–16957.

Schutte, J., Wang, H., Antoniou, S., Jarratt, A., Wilson, N.K., Riepsaame, J., Calero-Nieto, F.J., Moignard, V., Basilico, S., Kinston, S.J., et al. (2016). An experimentally validated network of nine haematopoietic transcription factors reveals mechanisms of cell state stability. Elife *5*, e11469.

Scialdone, A., Tanaka, Y., Jawaid, W., Moignard, V., Wilson, N.K., Macaulay, I.C., Marioni, J.C., and Gottgens, B. (2016). Resolving early mesoderm diversification through single-cell expression profiling. Nature *535*, 289–293.

Solaimani Kartalaei, P., Yamada-Inagawa, T., Vink, C.S., de Pater, E., van der Linden, R., Marks-Bluth, J., van der Sloot, A., van den Hout, M., Yokomizo, T., van Schaick-Solerno, M.L., et al. (2015). Whole-transcriptome analysis of endothelial to hematopoietic stem cell transition reveals a requirement for Gpr56 in HSC generation. J. Exp. Med. *212*, 93–106.

Subramanian, A., Tamayo, P., Mootha, V.K., Mukherjee, S., Ebert, B.L., Gillette, M.A., Paulovich, A., Pomeroy, S.L., Golub, T.R., Lander, E.S., et al. (2005). Gene set enrichment analysis: a knowledge-based approach for interpreting genome-wide expression profiles. Proc. Natl. Acad. Sci. USA *102*, 15545–15550.

Swiers, G., Baumann, C., O'Rourke, J., Giannoulatou, E., Taylor, S., Joshi, A., Moignard, V., Pina, C., Bee, T., Kokkaliaris, K.D., et al. (2013). Early dynamic fate changes in haemogenic endothelium characterized at the single-cell level. Nat. Commun. *4*, 2924.

Taoudi, S., Gonneau, C., Moore, K., Sheridan, J.M., Blackburn, C.C., Taylor, E., and Medvinsky, A. (2008). Extensive hematopoietic stem cell generation in the AGM region via maturation of VE-cadherin+CD45+ pre-definitive HSCs. Cell Stem Cell *3*, 99–108.

Tavian, M., Robin, C., Coulombel, L., and Péault, B. (2001). The human embryo, but not its yolk sac, generates lympho-myeloid stem cells: mapping multipotent hematopoietic cell fate in intraembryonic mesoderm. Immunity *15*, 487–495.

Teichweyde, N., Horn, P.A., and Klump, H. (2017). HOXB4 increases Runx1 expression to promote the de novo formation of multipotent hematopoietic cells. Transfus. Med. Hemother. *44*, 128–134.

Thambyrajah, R., Mazan, M., Patel, R., Moignard, V., Stefanska, M., Marinopoulou, E., Li, Y., Lancrin, C., Clapes, T., Moroy, T., et al. (2016). GFI1 proteins orchestrate the emergence of haematopoietic stem cells through recruitment of LSD1. Nat. Cell Biol. *18*, 21–32.

Ueno, H., and Weissman, I.L. (2006). Clonal analysis of mouse development reveals a polyclonal origin for yolk sac blood islands. Dev. Cell *11*, 519–533.

Wahlster, L., and Daley, G.Q. (2016). Progress towards generation of human haematopoietic stem cells. Nat. Cell Biol. *18*, 1111–1117.

Wang, Y., Yates, F., Naveiras, O., Ernst, P., and Daley, G.Q. (2005). Embryonic stem cell-derived hematopoietic stem cells. Proc. Natl. Acad. Sci. USA *102*, 19081–19086.

Wareing, S., Mazan, A., Pearson, S., Gottgens, B., Lacaud, G., and Kouskoff, V. (2012). The Flk1-Cre-mediated deletion of ETV2 defines its narrow temporal requirement during embryonic hematopoietic development. Stem Cells *30*, 1521–1531.

Webber, B.R., Iacovino, M., Choi, S.H., Tolar, J., Kyba, M., and Blazar, B.R. (2013). DNA methylation of Runx1 regulatory regions correlates with transition from primitive to definitive hematopoietic potential in vitro and in vivo. Blood *122*, 2978–2986.

Will, E., Speidel, D., Wang, Z., Ghiaur, G., Rimek, A., Schiedlmeier, B., Williams, D.A., Baum, C., Ostertag, W., and Klump, H. (2006). HOXB4 inhibits cell growth in a dose-dependent manner and sensitizes cells towards extrinsic cues. Cell Cycle *5*, 14–22.

Wilson, N.K., Foster, S.D., Wang, X., Knezevic, K., Schutte, J., Kaimakis, P., Chilarska, P.M., Kinston, S., Ouwehand, W.H., Dzierzak, E., et al. (2010). Combinatorial transcriptional control in blood stem/progenitor cells: genome-wide analysis of ten major transcriptional regulators. Cell Stem Cell *7*, 532–544.

Wilson, N.K., Miranda-Saavedra, D., Kinston, S., Bonadies, N., Foster, S.D., Calero-Nieto, F., Dawson, M.A., Donaldson, I.J., Dumon, S., Frampton, J., et al. (2009). The transcriptional program controlled by the stem cell leukemia gene Scl/Tal1 during early embryonic hematopoietic development. Blood *113*, 5456–5465.

Zovein, A.C., Turlo, K.A., Ponec, R.M., Lynch, M.R., Chen, K.C., Hofmann, J.J., Cox, T.C., Gasson, J.C., and Iruela-Arispe, M.L. (2010). Vascular remodeling of the vitelline artery initiates extravascular emergence of hematopoietic clusters. Blood *116*, 3435–3444.

Stem Cell Reports, Volume *10*

Supplemental Information

HOXB4 Promotes Hemogenic Endothelium Formation without Perturbing Endothelial Cell Development

Nadine Teichweyde, Lara Kasperidus, Sebastian Carotta, Valerie Kouskoff, Georges Lacaud, Peter A. Horn, Stefan Heinrichs, and Hannes Klump

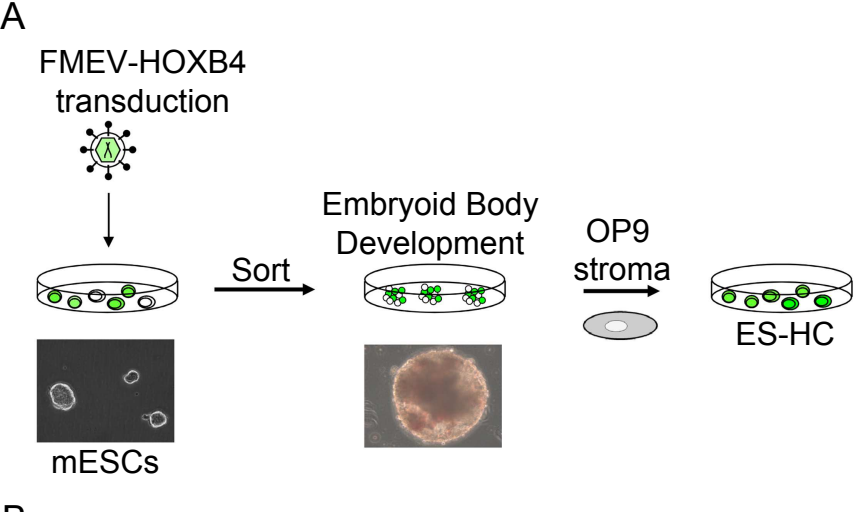
A
FMEV-HOXB4
transduction
Sort
Embryoid Body
Development
OP9
stroma
ES-HC
mESCs

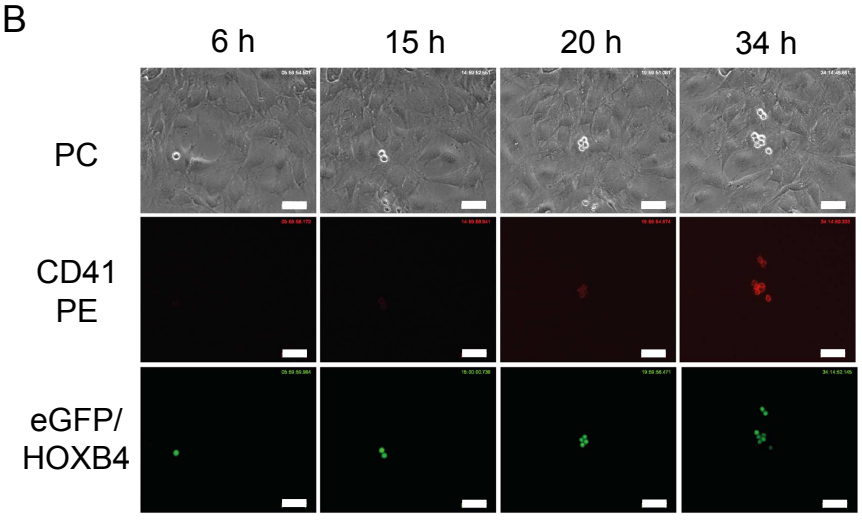
B
6 h
15 h
20 h
34 h
PC
CD41
PE
eGFP/
HOXB4

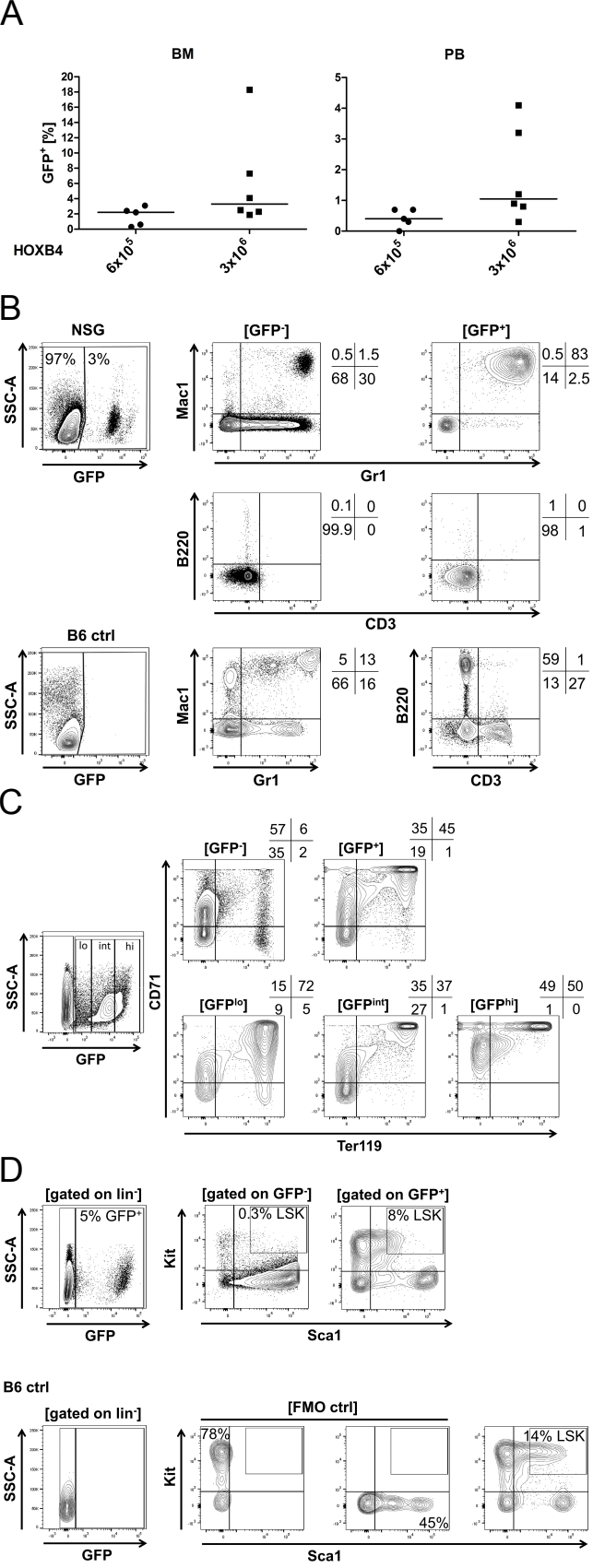
A
BM
PB
GFP+ [%]
HOXB4
6x10^5
3x10^6
B
NSG
B6 ctrl
[GFP-]
[GFP+]
SSC-A
GFP
Mac1
Gr1
B220
CD3
97%
3%
0.5 1.5
68 30
0.5 83
14 2.5
0.1 0
99.9 0
1 0
98 1
5 13
66 16
59 1
13 27
C
[GFP-]
[GFP+]
lo
int
hi
CD71
Ter119
57 6
35 2
35 45
19 1
[GFPlo]
[GFPint]
[GFPhi]
15 72
9 5
35 37
27 1
49 50
1 0
D
[gated on lin-]
[gated on GFP-]
[gated on GFP+]
5% GFP+
0.3% LSK
8% LSK
Kit
Sca1
B6 ctrl
[FMO ctrl]
78%
45%
14% LSK

A

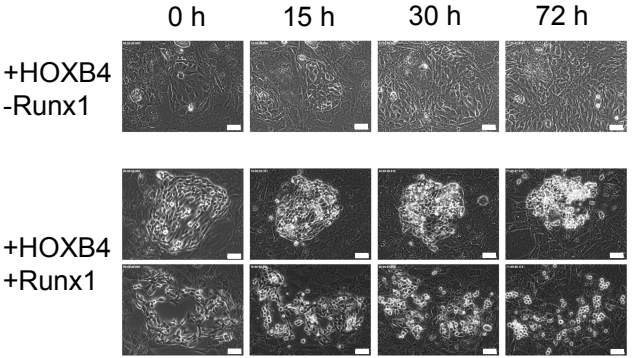
0 h
15 h
30 h
72 h
+HOXB4
-Runx1
+HOXB4
+Runx1

B

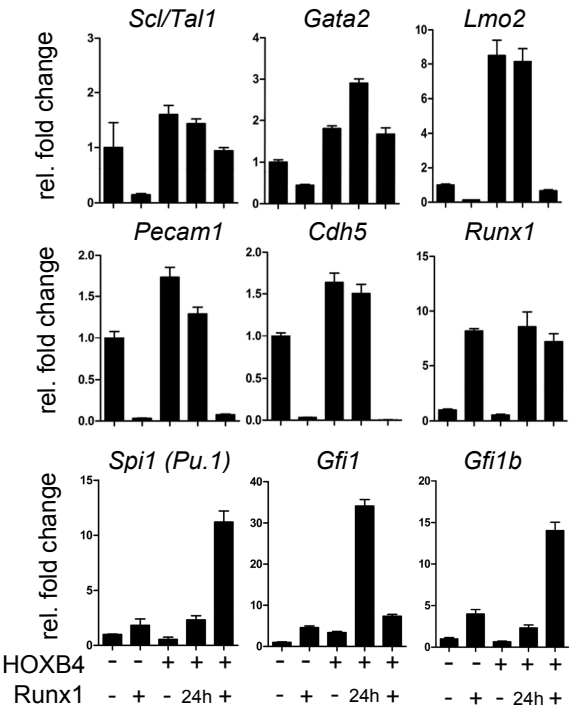
Scl/Tal1
Gata2
Lmo2
Pecam1
Cdh5
Runx1
Spi1 (Pu.1)
Gfi1
Gfi1b
rel. fold change
HOXB4
Runx1
24h

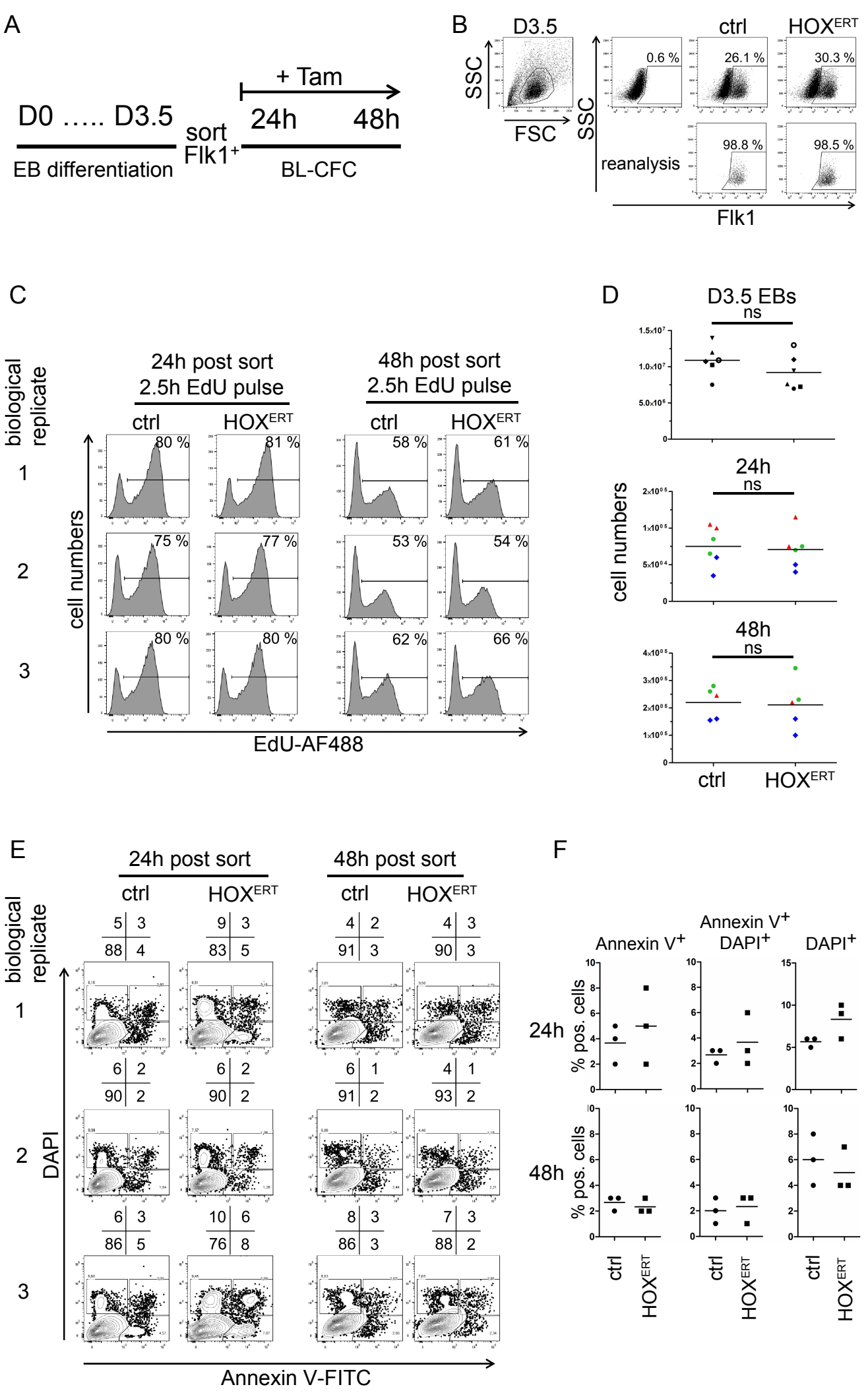
A
+ Tam
D0 ….. D3.5
24h
48h
sort
Flk1+
EB differentiation
BL-CFC
B
D3.5
ctrl
HOXERT
SSC
FSC
0.6 %
26.1 %
30.3 %
reanalysis
98.8 %
98.5 %
Flk1
C
biological replicate
24h post sort
2.5h EdU pulse
48h post sort
2.5h EdU pulse
ctrl
HOXERT
80 %
81 %
58 %
61 %
75 %
77 %
53 %
54 %
80 %
80 %
62 %
66 %
cell numbers
EdU-AF488
D
D3.5 EBs
ns
24h
ns
48h
ns
cell numbers
ctrl
HOXERT
E
24h post sort
48h post sort
ctrl
HOXERT
5 3 88 4
9 3 83 5
4 2 91 3
4 3 90 3
6 2 90 2
6 2 90 2
6 1 91 2
4 1 93 2
6 3 86 5
10 6 76 8
8 3 86 3
7 3 88 2
DAPI
Annexin V-FITC
F
Annexin V+
Annexin V+ DAPI+
DAPI+
24h
48h
% pos. cells
ctrl
HOXERT

Supplemental Information

Supplemental Figures and Videos

Figure S1. Development of hematopoietic progenitors from differentiating ESCs, Related to Figure 1.
(A) Retrovirally transduced ESCs were purified by flow cytometry based on fluorescent protein expression, differentiated as embryoid bodies, which were dissociated and cocultered on OP9 stroma cells. ES-HC: ES-cell derived hematopoietic cells. **(B**, **related to Movie S1)** Time lapse microscopy was used to follow upregulation of CD41 expression during hematopoietic differentiation of HOXB4-ESCs. 48 hour time lapse recording of single suspension cells expressing the FMEV-eGFP-2A-HOXB4 vector was initiated 5 days after placing dissociated d6EBs on OP9 stroma cells. A PE-labeled anti-CD41 antibody was added to the culture medium to detect initiation of CD41 expression (an example from n=5 independent experiments is shown). Scale bars: 50 µm.

Figure S2. HOXB4$^+$ ESC-derived hematopoietic progenitors mediate myeloid-biased repopulation in NSG-mice, *in vivo*, Related to Figure 2A.
Analysis of mice 6 weeks after transplantation with 6x10^5 or 3x10^6 GFP$^+$/HOXB4$^+$ CCE-cells, which were harvested after 6 days of embryoid body differentiation and subsequent co-culture on OP9 cells for further 14 days. **(A)** shows the overall percentages and median values of GFP$^+$HOXB4$^+$ cells in the bone marrow (BM) and peripheral blood (PB) of single transplanted mice. **(B-D)** Flow cytometric analysis of bone marrow from a representative mouse is shown, together with that from a C57/Bl6 control mouse (B6 ctrl). The proportions of lineage positive cells within GFP$^+$ or GFP$^-$ cell populations are indicated in the quadrant analysis next to the contour plots. **(B)** GFP$^+$/HOXB4$^+$ strongly skews repopulation towards MAC1(CD11b)$^+$GR1$^+$ myeloid cells and inhibits development of B220$^+$ B- or CD3$^+$ T-lymphoid cells. **(C)** Erythroid expression of TER119$^+$/CD71$^+$ is shown, gated on the expression levels of GFP$^+$/HOXB4$^+$. Because of the 2A^{esterase} based coexpression strategy, GFP-fluorescence directly correlates with HOXB4 expression levels (Klump et al., 2001; Will et al., 2006). HOXB4 inhibits erythroid differentiation in a dosage dependent manner, reflected by the lack of more mature TER119$^+$CD71^{lo} cells when HOXB4 is highly expressed (Chen et al., 2009; Koulnis et al., 2011). **D)** Bone marrow cells were gated on the lineage$^-$ (Lin$^-$) population and expression of Kit and Sca1 determined. The proportion of LIN$^-$SCA1$^+$KIT$^+$ (LSK) hematopoietic progenitor cells is indicated in the insets.

Figure S3. Endothelial-to-Hematopoietic Transition (EHT) of HOXB4$^+$ hemogenic endothelium, Related to Figure 2 and Movie S2.
(A) Dissociated iRunx EBd6 were placed on OP9 cells and cultured for 2 days prior to the induction of *Runx1* with 0.1 µg/ml doxycycline. Endothelial-to-hematopoietic transition (EHT) was documented from day 4 of *Runx1* induction on, with images taken every 10 minutes. Morphological changes of two individual colonies are shown from four time points of a 72 hour period (lower two rows). Scale bars: 50 µm. **(B)** qRT-PCR analysis showing the relative amounts of the indicated transcripts in the EBd6/OP9d4 cultures, +/- induction of HOXB4 throughout differentiation and +/- induction of *Runx1* either from day 3 of EB-development on or only for 24 hours between day 3 and day 4 of OP9 co-culture ("24h"). Values were normalized against *Actb* and *Gapdh* housekeepers. Expression was related to the controls without *Runx1* and HOXB4 induction. Columns represent arithmetic mean values of n=3 independent experiments, error bars represent standard deviations.

Figure S4: HOXB4 does not alter proliferative activity or apoptosis of FLK-1$^+$ progenitor cells, Related to Figure 5.
(A) Scheme of the experimental strategy. **(B)** 500,000 ESCs from each sample (ctrl and HOXB4^{ERT} without 4-Hydroxytamoxifen (Tam)) were used for EB differentiation. At day 3.5 of EB differentiation, FLK-1$^+$ cells were isolated by FACS and 50,000 cells placed into blast culture medium. A representative plot is shown. **(C)** 24 hours or 48 hours later, replicating DNA was labeled with EdU for 2.5 hours. After addition of Alexa Fluor 488 picolyl azide, the proportion of EdU-AF488 positive cells was determined by flow cytometry. The results of three independent, biological replicates are shown. **(D)** Total cell numbers of day 3.5 EBs and purified FLK-1$^+$ cells after 24 and 48 hours of growth in blast culture medium were determined. Biological replicates are depicted by different symbols, technical replicates by the same colors. Bars indicate arithmetic means of cell numbers. P values were calculated based on the two-sided, unpaired Student´s t-test. A P-value < 0.05 was considered statistically significant. **(E)** Proportions of Annexin V and/or DAPI positive cells were determined by flow cytometry after 24 and 48 hours growth of isolated FLK-1$^+$ cells. Quadrant analyses showing the percentages are given above each plot. Figure **(F)** summarizes the proportions of early apoptotic (Annexin V$^+$/DAPI$^-$), late apoptotic (Annexin V$^+$/DAPI$^+$) and dead (Annexin V$^-$/DAPI$^+$) cells after 24 and 48 hours. Bars represent arithmetic means of the percentages.

Table S1: Gene expression changes associated with HOXB4 expression, Related to Figure 6A,B.

Table S2: Gene sets used for GSEA, Related to Figure 6C.

Movie S1. Genesis of CD41$^+$ hematopoietic cells, *in vitro*, promoted by HOXB4, Related to Figure 1C.
Movie S1 shows an example of a suspension cell generated from differentiating HOXB4$^+$ CCE ESCs whose daughter cells upregulate CD41 expression indicating the genesis of very first hematopoietic cells, *in vitro*. 48 hour time lapse recording of single cells in suspension retrovirally coexpressing eGFP and HOXB4 was initiated 5 days after placing dissociated d6EBs on OP9 stroma cells. Images were taken in 15 min. intervals. A PE-labeled anti-CD41 antibody was added to the culture medium (final concentration: 20 ng/ml) to detect initiation of CD41 expression. **(A)** Fluorescence **(B)** Phase contrast. Scale bars: 50 µm.

Movie S2. Endothelial-to-Hematopoietic Transition of HOXB4$^+$ hemogenic endothelium, Related to Figure 2E.
Movie S2 shows the process of endothelial-to-hematopoietic transition (EHT) of HOXB4 expressing mouse iRunx ESC-derived endothelial circular sheets formed from day 4 of OP9 coculture on, +/- induction of *Runx1* expression. Phase contrast images were taken every 10 minutes. **(A)** without Runx1, **(B)** after *Runx1* induction. Scale bars: 50 µm.

Supplemental Experimental Procedures

Production of gammaretroviral particles
293T packaging cells were transfected in 175 cm^2 flasks with 15 µg of each FMEV-derivative together with 15 µg of a plasmid expressing MLV gag-pol and 6 µg of an expression plasmid encoding the VSV-G gene driven by the CMV promoter. Transfection was performed via the $Ca_3(PO_4)_2$ precipitation method. Cell culture supernatants containing the retroviral vector particles were collected after 24 and 48 hours. Titration of vector-containing supernatants was performed using 10^5 HT1080 fibroblasts.

ES-cell culture, retroviral transduction and embryoid body differentiation
Mouse embryonic stem cells were either grown in gelatin-coated flasks (CCE ES cells)(Pilat et al., 2013) or growth-arrested murine CF1-embryonic fibroblasts (iRunx ES cells) in knockout DMEM medium containing 15% ($^v/_v$) pretested fetal calf serum (FCS), 2 mM L-glutamine (L-Gln), $1.5x10^{-4}$ M Monothioglycerol (MTG) (Sigma-Aldrich, Taufkirchen, Germany), 10 ng/ml Leukemia Inhibitory Factor (LIF, R&D) and 1% ($^v/_v$) Penicillin/Streptomycin. For isolation and subsequent culture of retrovirally transduced, fluorescent ESCs, flow cytometrical sorting was performed using a BD FACSAria III (Beckton-Dickinson, USA). DMEM was exchanged for IMDM 2 days prior to initiation of *in vitro* differentiation. Embryoid body (EB) formation was performed in suspension, as previously described with slight modifications (Lesinski et al., 2012), after removal of MEFs by magnetic activated cell sorting (MACS; Feeder Removal MicroBeads mouse; Miltenyi Biotec, Bergisch-Gladbach, Germany). Briefly, 5000 ES-cells/ml were plated in IMDM medium (Lonza, Switzerland), 15% ($^v/_v$) fetal calf serum, 5% ($^v/_v$) Protein-Free Hybridoma Medium II (PFHM-II; Gibco, ThermoFisher Scientific), 2 mM L-Glutamine (L-Gln), 0.5% ($^v/_v$) Penicillin/Streptomycin (Sigma-Aldrich), 50 µg/ml ascorbic acid (Sigma Aldrich), 300 µg/ml iron saturated transferrin (Sigma-Aldrich), and $4x10^{-4}$ MTG. EBs were dissociated by 0.05% Trypsin-EDTA treatment at 37°C for 2-5 minutes. As soon as the solution started to become turbid, enzymatic activity was inhibited by addition of FCS and the EBs immediately mechanically dissociated by vigorous pipetting.

Antibodies used for Flow Cytometry Analysis and Cell Sorting
Differentiating ESCs were analysed by flow cytometry using the following fluorochrome-conjugated rat anti-mouse monoclonal antibodies, purchased from eBioscience/ThermoFisher (eBio) or BioLegend (BL):

specificity	provider	clone	conjugate	cat.no.
FLK-1 (CD309)	eBio	Avas12a1	APC	17-5821-80
FLK-1 (CD309)	eBio	Avas12a1	PE	12-5821-81
FLK-1 (CD309)	eBio	Avas12a1	Biotin	13-5821-81
TIE-2 (CD202b)	eBio	TEK4	PE	12-5987-81
TIE-2 (CD202b)	eBio	TEK4	Biotin	13-5987-82
TIE-2 (CD202b)	BL	TEK4	APC	124009
VE-Cadherin (CD144)	eBio	BV13	PE	12-1441-80
VE-Cadherin (CD144)	eBio	BV13	Biotin	13-1441-80

VE-Cadherin (CD144)	eBio	BV13	APC	17-1441-80
VE-Cadherin (CD144)	BL	BV13	BV 421	138013
CD41a	eBio	MWReg30	PE	12-0411-81
CD41a	eBio	MWReg30	Biotin	13-0411-82
CD41a	eBio	MWReg30	APC	17-0411-80
CD41a	eBio	MWReg30	APC-eFluor 780	47-0411-82
CD45	eBio	30-F11	PE-Cy7	25-0451-81
CD45	eBio	30-F11	Biotin	13-0451-81
CD45	eBio	30-F11	PE	12-0451-82
CD45	eBio	30-F11	APC	17-0451-82
CD45	BL	30-F11	BV 711	103147
KIT (CD117)	eBio	2B8	APC	17-1171-81
KIT (CD117)	eBio	2B8	PE-Cy7	25-1171-82
KIT (CD117)	BL	2B8	BV 421	105827
PDGFRB (CD140b)	eBio	APB5	PE	12-1402-81
PDGFRB (CD140b)	eBio	APB5	Biotin	13-1402-82
PDGFRA (CD140a)	eBio	APA5	Biotin	13-1401-80
PDGFRA (CD140a)	eBio	APA5	PE-Cy7	25-1401-82

For analysis of bone marrow and peripheral blood of transplanted mice, the following additional antibodies against surface markers were used:

specificity	**provider**	**clone**	**conjugate**	**cat.no.**
CD11b (MAC-1)	eBio	M1/70	PerCP-Cy5.5	45-0112-82
CD11b (MAC-1)	eBio	M1/70	APC	17-0112-82
CD150	BL	TC15-12F12.2	BV 421	115926
CD48	BL	HM48-1	PerCP-Cy5.5	103422
SCA1 (LY-6A/E)	eBio	D7	PE-Cy7	25-5981-82
B220 (CD45R)	eBio	RA3-6B2	PE-Cy7	25-0452-82
CD3ε	eBio	145-2C11	PerCP-Cy5.5	45-0031-82
CD3ε	BL	BM10-37	BV 421	100341
KIT (CD117)	eBio	2B8	APC	17-1171-82
CD71	BL	RI7217	PE-Cy7	113812
TER-119	eBio	TER-119	APC	17-5921-82
GR-1 (LY-6G)	eBio	RB6-8C5	eFluor 450	48-5931-82

For lineage cell detection in mouse bone marrow, the biotin-conjugated antibody cocktail was used from Miltenyi Biotec (Bergisch-Gladbach, Germany)(cat.no. 130-092-613).
Biotin-labeled antibodies were detected with Streptavidin conjugated to either APC-eFluor 780 (TF, cat.no. 47-4317-82) or PE-Cy7 (TF, cat.no. 25-4317-82).

Hematopoietic differentiation on OP9 cells
Dissociated EBs were cocultured with OP9 cells in IMDM, 10% ($^{v}/_{v}$) FCS (PAA/GE-Healthcare), 2 mM L-Gln containing the following cytokines: 100 ng/ml rmSCF, 40 ng/ml rmTPO, 100 ng/ml rhFlt3, 40 ng/ml rhVEGF (STFV)(McKinney-Freeman et al., 2009). All employed cytokines were obtained from PeproTech (Hamburg, Germany). OP9 stroma cells were plated at a density of 250,000 cells per 6-well 24 hours prior to cocultivation, in α-MEM (GE-Healthcare) supplemented with 20% ($^{v}/_{v}$) FCS (Biochrom), 2 mM L-Gln and 1% ($^{v}/_{v}$) Penicillin/Streptomycin. Cell numbers and volumes were determined using an electronic cell counter (CASY, Schärfe Systems, Reutlingen, Germany).

Hematopoietic Colony Assays
For testing the ability to form hematopoietic colonies, ESC-derived hematopoietic cells were plated in semisolid methylcellulose supplemented with rmSCF, rmIL-3, rhIL-6 and rhEPO (M3434 MethoCult, Stem Cell Technologies) in 24 wells by seeding 500 ESC-HCs. All assays were done in triplicates and colonies evaluated after 12 days.

Proliferation measurements
For measuring cell proliferation, incorporation of EdU (5-ethynyl-2'-deoxyuridine) into DNA during replication was determined. In brief, day 3.5 embryoid bodies from iRunx-ESCs (ctrl and HOXB4^{ERT} without Tamoxifen) were dissociated, 50,000 FLK-1^{+}cells isolated by FACS and seeded on gelatinized plates in IMDM containing 10% ($^{v}/_{v}$) FCS (GE-Healthcare), 2 mM L-glutamine, 20% ($^{v}/_{v}$) D4T conditioned medium, 1% ($^{v}/_{v}$) Penicillin/Streptomycin, 4.5x10^{-4} M MTG, 25 ng/ml ascorbic acid, 300 µg/ml holotransferrin (Sigma-Aldrich), 10 ng/ml rhIL-6, 5 ng/ml rhVEGF and Tam (100 nM). Cells were incubated under hypoxic conditions (3% O_2) at 37^{0}C in a H_2O saturated atmosphere. 24 and 48 hours post sort, cells were pulse-labeled for 2.5 hours after addition of 10 µM EdU to the medium. As a negative control, medium containing 0,1% (v/v) DMSO (the solvent used for the 10 mM EdU stock) was used. Incorporated EdU was detected by staining with Alexa Fluor 488 picolyl azide and subsequent analysis by flow cytometry, according to the according to manufacturer's recommendations (Click-it^{TM} Plus EdU Flow Cytometry Assay Kit, Thermo Fisher Scientific, Germany).

Apoptosis assay
The Annexin V-FITC kit (Miltenyi Biotec, Bergisch-Gladbach, Germany) in combination with DAPI staining was employed to determine the proportion of apoptotic and dead cells. EBd3.5 FLK-1^{+} iRunx cells were isolated and grown as described for the proliferation assay. On two consecutive days (24 and 48 hours post FLK-1^{+} sort), cells were stained with Annexin V-FITC and DAPI (final concentration 0.1 µg/ml). As a positive control for apoptosis, FLK-1^{+} sorted cells irradiated with 10 Gy were used.

Transplantation experiments and analysis
All animal experiments were approved by the Landesamt für Natur, Umwelt und Verbraucherschutz Nordrhein-Westfalen (LANUV)(reference number 84-02.04.2013.A350) and were performed according to official guidelines and regulations. 8-12 weeks old NOD.Cg-Prkdc^{scid}IL2rgtm1^{Wjl}/SzJ (NSG) mice were sublethally irradiated with 2 Gy and transplanted via retro-orbital injection. Prior to transplantation, OP9 stromal cells were removed using a monoclonal antibody directed against CD140b and subsequent MACS, according to the manufacturer´s guidelines (Miltenyi, Bergisch-Gladbach, Germany). 6x10^{5}, 3x10^{6} of unsorted ESC-derived hematopoietic cells were co-transplanted with 1x10^{5} freshly isolated, bone-marrow cells (NOD/SCID) per recipient mouse. For analysis, mice were sacrificed 6 weeks post transplantation. Total bone marrow cells were harvested from tibae and femora after crushing with pestle and mortar in MACS-buffer (1xDPBS, 0.5% BSA, 2 mM EDTA). After filtering through a 40 µm mesh (cell strainer, BD Bioscience), red blood cells were lysed with ACK lysing buffer (Lonza), for 8 min. on ice. Before flow cytometry analysis, whole bone marrow and peripheral blood samples were counted on an animal blood counter system (Scil VetABC hematology analyzer, animal care company, Viernheim, Germany). Lineage positive cells from BM were collectively labeled with biotinylated lineage marker antibodies (GR-1, CD11b, B220, CD3ε and TER119)(Miltenyi Biotec, Bergisch-Gladbach, Germany, cat.no. 130-092-613) and stained with Streptavidin-APC eFluor conjugate. Peripheral blood was obtained from mouse tail veins or from the retro-orbital sinus using heparin-coated capillary tubes. After erythrocyte lysis, cells were washed with 1xPBS, antibody staining performed in MACS-buffer.

Analysis of transcription by qRT-PCR
For quantitative, real-time PCR (qRT-PCR) measurements of gene specific transcripts, total RNA was extracted from cells using TRIzol reagent (Thermo Fischer Scientific Inc., Waltham, MA, USA) and subsequent purification of RNA using the RNeasy kit (Qiagen, Hilden, Germany). 1 µg of RNA were reverse transcribed into cDNA using a mixture of Oligo dT and random hexamer primers (QuantiTect Reverse Transcription Kit, Qiagen, Hilden, Germany). The RNA template was then removed with RnaseH and 1/100 volume of the reaction used for a PCR reaction using the following desoxyoligonucleotide-primers:

Runx1:	5´- ATGACCAGCCTCTCTGCAGAACT- 3´and
	5´-AGATGGACGGCAGAGTAGGGAA -3´
Gfi1:	5´- CTGTGCTAGGTATGGGAGAGCCAG-3´ and
	5´- GCCTTCTTCAGAACTCCCTTGGG -3´
Gfi1b:	5´- CAGGATGGGGAATCACCACTC -3´and
	5´- GGGGTCTGTGTGTAGCTGT -3´
Lmo2:	5´- GACGGAAATTGTGCAGGAG -3´ and
	5´- GATGCACAGAGACCATCCT -3´
Sox17:	5´- ACGCTAGCTCAGCGGTCTACTAT -3´and
	5´- AAGGATTTCCTTAGCGCTTCCAG -3´
Pu.1 (Sfpi1):	5´- AGCAGAGCTCAGATGAGGAGGAG -3´and
	5´- GGAACTGGTACAGGCGAATCTTT -3´
Scl/Tal1:	5´-CCAACAACAACCGGGTGAAG -3´ and

	5´-GCCGCACTACTTTGGTGTGAG- 3´
Gata2:	5´-GCTGCAGAGCACCCTAACCG -3´ and
	5´-CTTCTCTTATGCGGGTACTAGCAC -3´
Pecam1:	5´-AGCAATGGCAACTGGAGCGAGC -3´ and
	5´-TCTTCTTTGGGCCTTCGGCAT -3´
Cdh5:	5´-CCCAGGGCACACCTTGCAGAA -3´ and
	5´-CAAGGGAGAGATGCAGAGAGGC -3´

The amplification efficiency of each primer pair was determined as described (Pfaffl, 2001). Amplification was carried out in 96-well PCR plates (Peqlab/VWR, Erlangen, Germany) in a Biorad CFX real-time-PCR machine, using the QuantiFast SYBRGreen reagents (Qiagen, Hilden, Germany). Relative differences in gene expression were calculated using the $2^{-\Delta CT}$ method by normalizing the CT-values for each gene to the CT-values of two housekeeping genes, *β-Actin* and *Gapdh* (Vandesompele et al., 2002). Cycling conditions were 95^0C for 5 min followed by 40 amplification cycles being 95^0C denaturation for 10 sec and a combined annealing and elongation step at 60^0C for 30 sec.

Time Lapse Microscopy

For time lapse analysis, cultures were kept at 37^0C, 5% CO_2, 3% O_2 in a humidified chamber (Incubator XL multiS1, Zeiss, Jena, Germany). Photos were taken using a Zeiss Axio Observer X.1 microscope. Axio Vision Software 4.8 was used for image processing, editing and animation (Carl Zeiss, Jena, Germany). For detection of CD41 expression on the cell surface of emerging hematopoietic cells, phase contrast and fluorescence images were taken in 15 minute intervals from day 5 of OP9 coculture on, over a 48 hour period. The PE-conjugated anti-CD41 mAb was directly added to the culture medium every 8 hours at a final concentration of 20 ng/ml (Movie S1A). For documentation of EHT, phase contrast photos of iRunx/OP9 cocultures were taken in 10 minute intervals, from day 4 of coculture on over a period of 72 hours. For induction of *Runx1* and documentation of ongoing EHT, doxycycline was added to the cultures on day 2 and day 4 of OP9 coculture in a final concentration of 0.1 µg/ml (Movie S1B).

References:

Chen, K., Liu, J., Heck, S., Chasis, J.A., An, X., and Mohandas, N. (2009). Resolving the distinct stages in erythroid differentiation based on dynamic changes in membrane protein expression during erythropoiesis. Proc Natl Acad Sci U S A *106*, 17413-17418.

Klump, H., Schiedlmeier, B., Vogt, B., Ryan, M., Ostertag, W., and Baum, C. (2001). Retroviral vector-mediated expression of HoxB4 in hematopoietic cells using a novel coexpression strategy. Gene Ther *8*, 811-817.

Koulnis, M., Pop, R., Porpiglia, E., Shearstone, J.R., Hidalgo, D., and Socolovsky, M. (2011). Identification and analysis of mouse erythroid progenitors using the CD71/TER119 flow-cytometric assay. J Vis Exp. *54*, 2809.

Pilat, S., Carotta, S., and Klump, H. (2013) Development of hematopoietic stem and progenitor cells from mouse embryonic stem cells, in vitro, supported by ectopic human HOXB4 expression. Methods Mol Biol *1029*, 129-147.

Pfaffl, M.W. (2001). A new mathematical model for relative quantification in real-time RT-PCR. Nucleic Acids Res *29*, e45.

Will, E., Speidel, D., Wang, Z., Ghiaur, G., Rimek, A., Schiedlmeier, B., Williams, D.A., Baum, C., Ostertag, W., and Klump, H. (2006). HOXB4 inhibits cell growth in a dose-dependent manner and sensitizes cells towards extrinsic cues. Cell Cycle *5*, 14-22.